

REPORT DOCUMENTATION PAGE

Form Approved OMB No. 0704-0188

Public reporting burden for this collection of information is estimated to average 1 hour per response, including the time for reviewing instructions, searching existing data sources, gathering and maintaining the data needed, and completing and reviewing the collection of information. Send comments regarding this burden estimate or any other aspect of this collection of information, including suggestions for reducing this burden to Washington Headquarters Services, Directorate for Information Operations and Reports, 1215 Jefferson Davis Highway, Suite 1204, Arlington, VA 22202-4302, and to the Office of Management and Budget, Paperwork Reduction Project (0704-0188), Washington, DC 20503.

1. AGENCY USE ONLY (Leave blank)		2. REPORT DATE 1997	3. REPORT TYPE AND DATES COVERED Final Report	
4. TITLE AND SUBTITLE Mid-Infrared Diode Lasers On III-V Alloys For The Spectral Range 3-3.5 Microns Operating Near Room Temperature			5. FUNDING NUMBERS F6170896W0078	
6. AUTHOR(S) Dr. Yuri Yakovlev				
7. PERFORMING ORGANIZATION NAME(S) AND ADDRESS(ES) Russian Academy of Sciences Politekhnickeskaya st. 26 St. Petersburg 194021 Russia			8. PERFORMING ORGANIZATION REPORT NUMBER N/A	
9. SPONSORING/MONITORING AGENCY NAME(S) AND ADDRESS(ES) EOARD PSC 802 BOX 14 FPO 09499-0200			10. SPONSORING/MONITORING AGENCY REPORT NUMBER SPC 96-4006	
11. SUPPLEMENTARY NOTES				
12a. DISTRIBUTION/AVAILABILITY STATEMENT Approved for public release; distribution is unlimited.			12b. DISTRIBUTION CODE A	
13. ABSTRACT (Maximum 200 words) This report results from a contract tasking Russian Academy of Sciences as follows: The contractor will investigate new physical approaches for designing middle infrared diode lasers operating near room temperature in the spectral range 3-3.5 microns. The contractor will employ two different approaches improved laser structures based on InAsSb/InAsSbP alloys and non-traditional tunnel laser structures. The contractor will compare the performance of the various types of the diode lasers developed in the US. The contractor will deliver one interim report and one final report. The contractor will also deliver at least one broad stripe laser demonstrating high power and at least one laser demonstrating high temperature (near room temperature) operation.				
14. SUBJECT TERMS Lasers			15. NUMBER OF PAGES 52	
			16. PRICE CODE N/A	
17. SECURITY CLASSIFICATION OF REPORT UNCLASSIFIED	18. SECURITY CLASSIFICATION OF THIS PAGE UNCLASSIFIED	19. SECURITY CLASSIFICATION OF ABSTRACT UNCLASSIFIED	20. LIMITATION OF ABSTRACT UL	

19980102 019

DTIC QUALITY INSPECTED 4

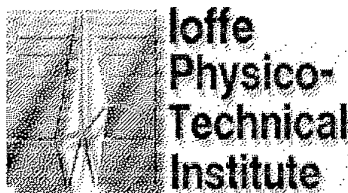
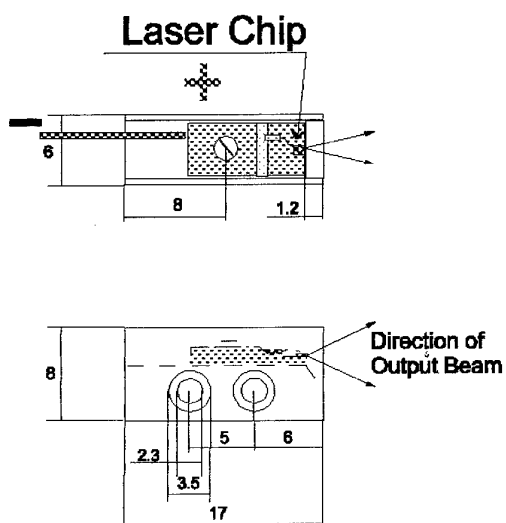
Diode Laser LD 32

Serial Number V12041

(broad stripe laser)

PARAMETER	UNITS	CONDITIONS	RATINGS
WAVELENGTH, λ	μm	T=77 K	3.284 @ 1.1 I_{th}
THRESHOLD CURRENT, I_{th}	mA	CW operation	140 @ 77 K
MAXIMAL DIRECT CURRENT	I_{th}	@ 77 K	3.5
ELECTRICAL MODULATION	Hz	@ 77 K	20-400
CHINK	times	@ 77 K	2
MODE STRUCTURE		CW	multi
STRIPE WIDTH	μm		90
CAVITY LENGTH	μm		625
DATE	V.Sherstnev 20.03.97 sherstnev@iropt7.ioffe.rssi.ru		

IMPORTANT: PLUS - ON CASE
MINUS - ON WIRE



Politekhnikeskaya 26
194021 St. Petersburg,
Russia

Phone: (812) 247 99 56
Fax: (812) 247 00 06

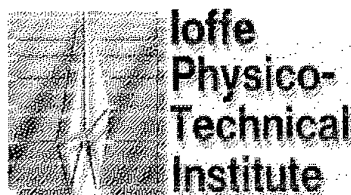
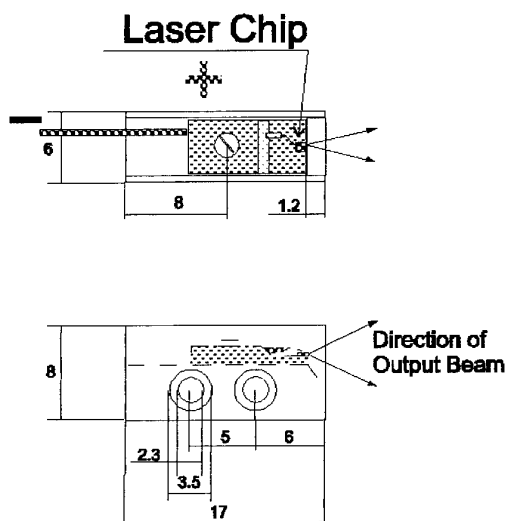
Diode Laser LD 32

Serial Number V12192

(high temperature laser)

PARAMETER	UNITS	CONDITIONS	RATINGS
WAVELENGTH, λ	μm	T=77 K	3.272 @ 1.1 I_{th}
THRESHOLD CURRENT, I_{th}	mA	CW operation	28 @ 77 K
OPTICAL POWER, P_{out}	mW	@ 77 K, 2 I_{th}	2.0
MODE STRUCTURE		CW	single
OPERATION TEMPERATURE	K		77-200
MODE TUNING	cm^{-1}/K	average	1.2
CAVITY LENGTH	μm		300
DATE	V.Sherstnev 20.03.97 sherstnev@iropt7.ioffe.rssi.ru		

IMPORTANT: PLUS - ON CASE
MINUS - ON WIRE



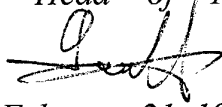
Politekhnicheskaya 26
194021 St. Petersburg,
Russia

Phone: (812) 247 99 56
Fax: (812) 247 00 06

Final Report

EOARD Contract F 61708-96-W0078

Mid-Infrared Diode Lasers on III-V Alloys for the Spectral Range $3\div 3.5\text{ }\mu\text{m}$ Operating Near Room Temperature: New Physical Approaches

Principal Investigator *Yury P. Yakovlev, Dr.Sci., Head of Infrared Optoelectronics Laboratory*  21/02/97

Work period *12 months (February 21, 1996 - February 21, 1997)*

*Ioffe Physical Technical Institute
Russian Academy of Sciences
Saint Petersburg
Russia*

Project manager: Yury P. Yakovlev, Dr.Sci., Head of infrared optoelectronic laboratory

Key persons:

Maya P. Mikhailova, Deputy P.I., Dr. Sci., l.r.s.

Albert N. Imenkov, Dr. Sci., l.r.s.

Georgy G. Zegrya, Dr. Sci., s.r.s.

Investigators:

Tamara N. Danilova, Ph.D., r.s.

Victor V. Sherstnev, Ph.D., r.s.

Konstantin D. Moiseev, Ph.D., r.s.

Victor A. Solov'ev, Ph.D., s.r.s.

Andrei A. Popov, Ph.D., r.s.

Oleg G. Ershov, j.r.s.

l.r.s. - *leading research scientist*

s.r.s. - *senior research scientist*

r.s. - *research scientist*

j.r.s. - *junior research scientist*

Content

Abstract

1. Introduction and overview
2. Program objective
3. Technical schedule
4. The creation and study of laser structures based on type I and type II InAs(Sb)InAsSbP GaInAsInGaAsSb heterojunctions.
 - 4.1. LPE growing of lattice matched laser structures.
 - 4.2. X-ray diagnostics and EBIC studying InAs-based lasers.
 - 4.3. Suppression of Auger- recombination in the diode lasers based on type II InAsSb/InAsSbP heterojunctions.
 - 4.3.1. Theoretical consideration.
 - 4.3.2. Experimental methods.
 - 4.3.3. Results and discussion.
5. CW high-power InAsSb/InAs/InAsSbP diode lasers for 3.4–3.6 μm spectral range.
 - 5.1. Experimental methods.
 - 5.2. Basic electrical characteristics of lasers.
 - 5.3. Threshold current characteristics of lasers.
 - 5.4. Power-current characteristics.
 - 5.5. Multi-mode and single-mode InAsSb lasers.
 - 5.6. Long term stability of 3.4 μm laser performance.
6. Theoretical analysis of the non-radiative losses in the longwavelength quantum well lasers (leakage current, Auger-recombination, intravalence band absorption, effect of heating).
7. Advanced type II broken-gap p-InAs_{0.17}AsSb/n-In_{0.83}GaAsSb heterolaser.
 - 7.1. Electroluminescence study of the type II broken-gap p-GaInAsSb/n-InAs heterojunction.
 - 7.2. Tunneling-injection laser ($\lambda=3.2\mu\text{m}$) with improved temperature characteristics of the threshold current.
8. AlGaAsSb/InAs double heterostructure with improved electron confinement.
 - 8.1. Growing AlAsSb/InAs DHs.
 - 8.2. Spontaneous emission and superluminescence in AlGaAsSb/InAs/AlGaAsSb heterostructure.
9. Comparative study of various types of InAs(Sb)/InAsSbP and GaInAsSb/InGaAsSb based laser structures. Comparison with state-of-the-art mid-infrared lasers.

Conclusion and outlook.

References.

Abstract

This work is devoted to using new physical approaches for design high temperature III-V mid-infrared diode lasers operating in the spectral range 3-3.5 μm . Simple and reproducible liquid-phase technology was developed for fabrication of InAs(Sb)/InAsSbP and GaInAsSb/InGaAsSb heterolasers. A great attention is paid to creation and detailed study of continuous wave high power InAsSb-based lasers. Good spectral, mode and tuning performances were achieved at $T=77\text{-}122\text{K}$. These CW single mode lasers are very promising for tunable diode laser spectroscopy and ecological monitoring. Theoretical analysis of main factors limiting high temperature operation of longwavelength quantum well lasers was performed. Contributions of non-radiative Auger recombination process, intervalence band absorption, effect of overheating and current leakage were discussed. Effect of overheating is considered and some experimental data are represented on the example of laser with GaInAsSb active layer. Evidence of Auger-recombination suppression was obtained in type II InAsSb/InAsSbP lasers with high band offsets ratio ($\Delta E_v/\Delta E_c \sim 3$).

High temperature (up to 220K), single mode pulse operation with characteristic temperature $T_0=40\text{K}$ and low threshold current were made and studied.

Advanced tunneling injection laser with type II broken-gap p-GaInAsSb/n-InAsSbP heterojunction in an active region was proposed and realized. Reduction of threshold current temperature dependence was observed in the range of 77-150K with $T_0=47\text{K}$ and operation temperature $T=200\text{K}$ were achieved. It was concluded that it is due to suppression of Auger-recombination and intravalence band absorption on the type II heterointerface.

In conclusion some prospective ways of further improving of mid-infrared laser performance are proposed.

1. Introduction and overview

Semiconductor lasers in the 3-4 μm wavelength region have been developed for a number of spectroscopic applications. As sources of narrow spectral bandwidth optical radiation these lasers give important access to the mid-infrared wavelengths where important molecules have fundamental absorption bands lie. A number of gases (such as CH_4 , H_2CO , CO , CO_2 , H_2O , SO_2 , NO_2 , and NO) [1] have strong absorption bands in the mid-infrared spectral region which are in 50-500 times stronger in comparison to near infrared overtone bands. With using mid-

infrared lasers a detection limit in terms of volume mixing ratio in the order of 10^{-10} - 10^{-12} can be achieved by tunable diode laser absorption spectroscopy (TDLAS)² technique in atmospheric chemistry, trace gas analysis, medical diagnostic and technological process control. For these ultra-sensitive concentration measurements the laser sources should have appropriate spectral and operating characteristics.

(1) CW operation in combination with possibility of frequency modulation (FM) is important to obtain low detection limits and a high temporal resolution in TDLAS. This is a problem because pumping by current with 100 % duty cycle of narrow band gap materials leads to a strong junction overheating. (2) Single mode lasing with suppression of side modes as high as 30 dB is required. Such suppression ratio will minimize mode portion noise and prevent a false absorption signal from side modes. (3) The CW output power should be at least 1 mW. At the case the laser power after transmitting through a multi-reflection absorption cell will generate a shot noise current above the thermal noise of commercial available photodetectors in the mid-infrared. (4) The laser should run at a temperature range closed to room temperatures or to liquid Nitrogen (LN_2), but not between. Only in this case continuous and routine measurements over long time periods are possible. (5) For shot noise limited frequency region the relative intensity noise (RIN) of the laser should be lower than -120 dB. The relaxation oscillation frequency of the laser should be higher than the 500 MHz. (6) The wavelength current and temperature tuning rates should be less than 1 GHz/mA and 30 GHz/Ke mode suppression to minimize frequency fluctuations caused by current controller and temperature driver noise, respectively. (7) A high long-term stability and low drift of the laser wavelength is required for routine and reproducible measurements.

Research in the field of mid-infrared lasers nowadays is being conducted in a number of scientific groups in the world such as Hughes Research Labs.³, Sandia National Lab.⁴, the Sarnoff Research Center^{5,6}, AT&T Bell Lab.^{7,8}, MIT Lincoln Lab.⁹⁻¹², Laser Photonics Inc.^{13,14} in the US, Fraunhofer Institute IPM¹⁵ in Germany and the Ioffe Institute St.Petersburg. and the Lebedev Institute in Moskow Russia. About 8 mW power has been obtained with long-pulsed injection InAsSb lasers¹⁷ at 3.2 μm . 2.7 mW pulsed optical power (only 1 % duty cycle) and single mode emission has been achieved from multiple quantum well (MQW) with GaInAsSb barriers and type-II GaInAsSb/InAs superlattice wells³.

Unfortunately these pulsed diodes can not be applied in real spectroscopic devices. Very promising results have been obtained with optical pumping. CW output powers of up to 16 mW has been observed from a 4 μm InAsSb laser optically pumped by a 2 μm laser, to avoid junction overheating [9]. A peak power of 0.54 W has been obtained for pulse operation with 58 W laser pumping [11]. However, direct wavelength modulation of optically pumped diodes is still a

problem. Recently high performance and maximum CW operation temperature of 175 K was achieved [12] for strained MQW lasers consisting of comparatively strained InAsSb active layers and tensile strained InAlAsSb barrier layers. They have exhibited CW powers of 4 mW. Up to 11 mW CW power with 3.6 μm injection laser was reported at [18]. However output power in these CW injection diodes has distributed over a number of modes. And mostly of the diodes can not be applied to spectroscopic applications.

Between mid-ir diode lasers, room temperature multimode pulse operation was reached only for GaInAs/InAlAs intersubband quantum cascade lasers (QCLs) [7]. It was a great breakthrough that opens the way to other room temperature mid-infrared diode lasers. But this unique QCL has some disadvantages. First, its technology is very complicated and expensive to be used for commercially available laser structures. Then, due to peculiarities of the superlattice absorption and rigid laser design proposed QCL can operate only at discrete wavelengths (at $\lambda=5.2$ and 8 μm) Third, they have shown CW lasing was up to 110 K only [7,8]. Besides, a wavelength tuning in QCLs is rather difficult due to its rigid design and strongly determined radiative recombination transitions between electron levels in quantum wells.

The lead-salts diodes for the 3 μm spectral region are not expected to obtain high CW power due to their thermal conductivity and under strong direct current and then by the III-V semiconductors are superior. PbEuSeTe/PbSnTe lasers [13] have been developed to meet TDLAS requirements. A tuning rate of 1.1-2.1 GHz/mA has been achieved at 4.3 μm wavelength but the output power was only 180 μW under 30 I_{th} [14]. For the 3-5 μm range optical power output of about 1.2 mW under strong ($\sim 30 \cdot I_{\text{th}}$) injection currents has been achieved for multi-mode PbEuSeTe/PbSe diode lasers grown by MBE, but their single mode CW power was below 300 μW ¹⁵.

A limited amount of publications dedicate to high spectral performance lasers. Mid-infrared InAsSb lasers operating at low LN_2 temperature have been fabricated specially for spectroscopic applications in Ioffe institute [20,21] and good tuning performances were demonstrated.

Further progress in improving mid-IR laser performances are connected with new physical approaches for developing and optimizing laser design as well as with more deep understanding physical reasons limited high temperature operation of mid-IR lasers.

Last two years there is a great current interest to novel types of mid-infrared lasers, especially quantum cascade lasers [7,8] and type II heterostructure and superlattice lasers [4,6]. Hughes Research Lab. investigators realized mid-infrared

laser grown by MBE employing GaInSb/InAs superlattice active regions and InAs/AlSb SL cladding layers. Emission wavelength of 3.18 μm at 255 K was reported on CLEO-96.

Type II broken-gap based laser structures are remaining now very intensively studying and promising devices. They allow to combine some features of both traditional and quantum cascade lasers as to possibility wavelength tuning and to "cascade" laser structure [16]. Then, weaker temperature dependence of the threshold current can be reached in these devices using the intersubband transitions and a possibility to suppress non-radiative losses at the interface.

Non-radiative Auger-recombination, intravalence band absorption of free carriers and leakage current due to carrier heating are main factors which do not permit to obtain lasing up to room temperature in longwavelength diode lasers.

In the frame of this work a great attention was paid to overcoming above mention problems. Lasers with modified design, both traditional ones and type II tunneling-injection one were proposed. Auger-recombination rate, intravalence band absorption, carrier heating and threshold current temperature dependence were examined both theoretically and experimentally. It allowed to improve some performances of the laser structure under study. Then a great part of this research work was devoted to creation of CW high power single mode mid-infrared lasers based on InAsSb(P) alloys.

2. Program Objective

The main objective of this one-year proposal is further increasing operation temperature of InAs-based mid-infrared lasers up to near room temperature by using new physical approaches. We propose two approaches for solving main goal of the project:

1. Improving traditional InAsSb/InAsSbP double heterostructure laser. This way includes:
 - 1.1. Buried-channel technology will be developed especially for laser structures based on the narrow-gap InAs solid solutions for reduction in surface leakage and threshold currents.
 - 1.2. Additional confinement layers based on GaAlAsSb will be used to improving electron confinement of traditional laser structures.

Additional aims of this work are to create CW high power single mode operating lasers, especially, for diode laser spectroscopy applications, and increasing output optical power of the broad-area lasers.

2. Further developing and improving non-traditional tunnel-injection laser structures on the base of type II broken /or near broken-gap GaInAsSb/InAs (InGaAsSb) heterojunctions. It will require the following tasks to be solved during:
 - 2.1. Studying tunnel injection lasers mechanism at type II heterointerface.
 - 2.2. Theoretical and experimental studying both radiative and non-radiative Auger recombination processes at p-p or p-n type II heteroboundary as well as threshold current and quantum efficiency temperature dependence.
 - 2.3. Theoretical studying and comparing the efficiency of various channels of non-radiative Auger recombination at type II p-p and p-n heterointerface. Analysis of Auger-recombination suppression mechanisms at type II p-p or p-n heterojunction.
 - 2.4. Theoretical analysis and calculation leakage currents through p-p and p-n heterojunction to evaluate limit operating temperature.
 - 2.5. Optimizing laser design, including active and confined layers, and experimental determination of limit lasing temperature for tunnel injection laser.

Various kinds of the lasers, developed in the frame of this proposal, both traditional and non traditional, will be compared in the point of view high-temperature limit of lasing.

Main result of the project will be design mid-infrared lasers, including single-mode ones. operating in the spectral range of 3-3.5 μm up to 230-250 K in pulse regime.

3. Technical schedule (February 21, 1996- February 21, 1997).

- I. Fabrication of buried-channel and broad-area lasers and tunnel-injection on the InAs base heterostructures (February 1996-April 1996)
 - 1.1. Developing buried-channel technology for InAs-bailed heterostructures. Fabricating buried- channel laser structures.
 - 1.2. Fabricating of broad-area laser structures based on InAs/InAsSb/InAsSbP.
 - 1.3. LPE growing novel laser structures with type II GaInAsSb/InAs (InGaAsSb) single heterojunctions in an active layers and InAsSbP confined layers. Fabrication of mesa-stripe laser structures.

- 1.4. X-ray diagnostic of laser structures, EBIC (electron beam induced currents studying of heterointerface location for both lasers of pp. 1a) and 1b)
1a,1b,1c: 1d.

II. Studying of buried-channel, broad area and tunnel injection laser structures (May-August 1996)

- 1.1. Investigation of current-voltage and intensity-current characteristics, spontaneous and coherent emission, and temperature dependence of threshold current for buried and broad- area lasers in the range of $T=77-300$ K.
- 1.2. Theoretical and experimental studying of leakage current in dependence on parameters of the various laser structures.
- 1.3. Investigation of current-voltage and intensity-current characteristics, spontaneous electroluminescence, losing characteristics, and temperature dependence of the threshold current for the tunnel-injection lasers in the range of $T=77-300$ K.
- 1.4. Theoretical calculation of radiative and non-radiative Auger-recombination rates and temperature dependence of the threshold current for tunnel-injection laser. Analysis of possible mechanism of Auger recombination suppression at p-p (p-n) type II heteroboundary.
2a→2b, 2c→2d.

III quarter (September - November 1996). Growing and studying InAs based laser structures with additional wide-gap cladding layers.

3a. LPE growing InAs/InAsSb/InAsSbP laser structures with additional Al-content cladding layers.

3b. Studying current-voltage and intensity-current characteristics and temperature dependence of the threshold currents for lasers with additional cladding layers. Comparison lasers with/or without additional confined layers.

3c. Theoretical evaluation of the optical losses limiting output power of the broad area lasers.

3d. Theoretical calculation of leakage currents through the p-p and p-n type II heterointerface in the tunnel-injection lasers.

3e. Optimization of the tunnel-injection laser structure.

3a->3b->c: 3d->3e.

IV quarter (December 1996 - February 1997). Comparative studying of various diode laser structures: buried-channel lasers, lasers with additional cladding layers and tunnel-injection lasers concerning to limit operating temperature.

4a. Theoretical analysis and calculation of limit operating temperature for various types of lasers under study: buried lasers, lasers with additional cladding layers and tunnel injection lasers. Comparison with referred laser structures.

4b. Comparative study the temperature dependence of the threshold current in pulse and cw mode for InAsSb/InAsSbP buried channel lasers and GaInAsSb/InAs tunnel-injection lasers.

4a->4b.

4. The creation and study of laser structures based on type I and type II InAs(Sb)/InAsSbP GaInAs/InGaAsSb heterojunctions.

4.1. LPE growing lattice matched laser structures.

Laser structures were grown by LPE on InAs(100) substrata with hole concentration $p = 2 \cdot 10^{18} \text{ cm}^{-3}$ at $T = 570\text{-}600^\circ\text{C}$. Cladding layers of p-InAsSb_{0.17}P_{0.35} ($E_g = 595 \text{ meV}$) were doped by Zn up to $p = 1\text{-}2 \cdot 10^{18} \text{ cm}^{-3}$ and their thickness was $d = 2.5\text{-}3 \text{ }\mu\text{m}$. Undoped active layer of InAsSb_x ($x = 0.03\text{-}0.07$) with $p = 2\text{-}5 \cdot 10^{16} \text{ cm}^{-3}$. Their composition and lattice-matching were also determined by X-ray diagnostic.

Energy band gap of active layers was in the range $E_g = 361\text{-}391 \text{ meV}$ and corresponds to emission range of $3\text{-}3.5 \text{ }\mu\text{m}$. Thickness of active layers was in the range of $d = 0.5\text{-}0.8 \text{ }\mu\text{m}$. Confined layers of n-type InAsSbP (P is 35%) were doped by Sn up to $p = 5\text{-}8 \cdot 10^{18} \text{ cm}^{-3}$ and had a thickness of $2.5\text{-}3 \text{ }\mu\text{m}$. Ohmic contacts were made from Au:Ge (p-layers) and Au:Te (n-layers) alloys by vacuum deposition and by fusion in H_2 atmosphere at $T = 350^\circ\text{C}$.

Electroluminescence was measured to control a quality of InAsSb/InAsSbP double heterostructures.

In the frame of this work an unique method was developed for analysis of the narrow-gap semiconductor homo- and heterostructures using scanning electron microscopy. It was described before in [4*].

In the case of multilayer heterostructures the precise measurement of p-n junction position relatively to the specific heterointerface becomes very important. For p-n junction location measurements of electron beam induced current (EBIC) mode in a scanning electron microscope (SEM) was used. Our investigations shown that the identification and precise measurement of position of the interfaces at InAs-based heterostructures is not trivial.

We have studied the specific features of signal formation in secondary electron (SE) and backscattering electron (BSE) modes. These modes are mostly used in SEM for characterization of layers with different chemical composition. Two types of structures were investigated:

4.2. X-ray diagnostics and EBIC study of LPE grown laser structures.

LPE grown laser structures were controlled by X-ray diagnostics to determine a solid solution composition in an active (InAsSb) and confined (InAsP and InAsSbP) layers. Microanalyzer CAMEBAX Microbeam was employed. For p-n junction location measuring in the both type of laser structure under study (InAsSb/InAsSbP and GaInAsSb/InGaAsSb/InAsSbP heterostructures) effective and precise method of electron beam induced current (EBIC) was applied which was developed in Ioffe Institute [4*].

It is known that narrow-gap heterostructures have large leakage current at room temperature. It does not allow in many cases to record EBIC (Electron Beam Induced Current) signal. Signal/noise ratio at room temperature is much smaller than at low temperature (near 77K). EBIC measurements at $T=81\text{K}$ allow to determine p-n junction location with high accuracy. By using this method an evaluation of diffusion lengths and interface recombination rates can be made at laser operation temperature.

Two type of heterostructures were analyzed by this method: traditional InAsSbP/InAsSb laser structure (Fig.1) and novel type-II broken-gap laser structure with p-GaIn_{0.17}AsSb/n-In_{0.84}GaAsSb heterojunction in active layer (Fig.2).

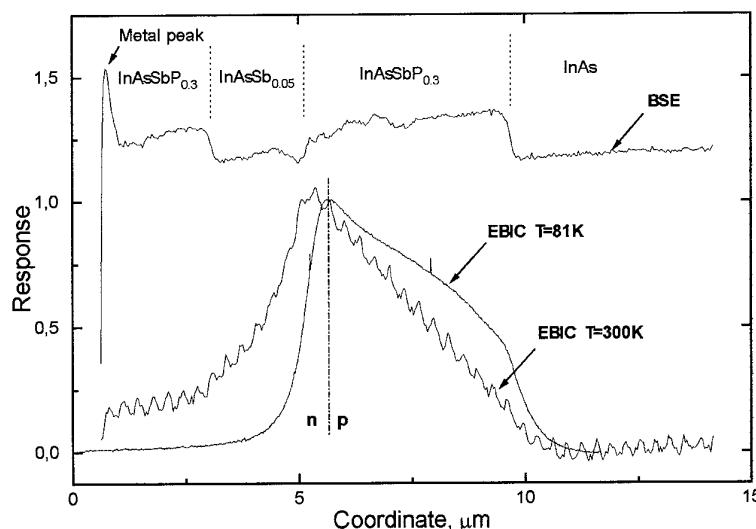


Figure 1 Backscattered electrons (BSE) and electron beam induced current (EBIC) line profiles at temperatures $T=81\text{K}$ and 300K for InAsSbP_{0.3}/InAsSb_{0.05} structure. Acceleration voltage - 10 kV.

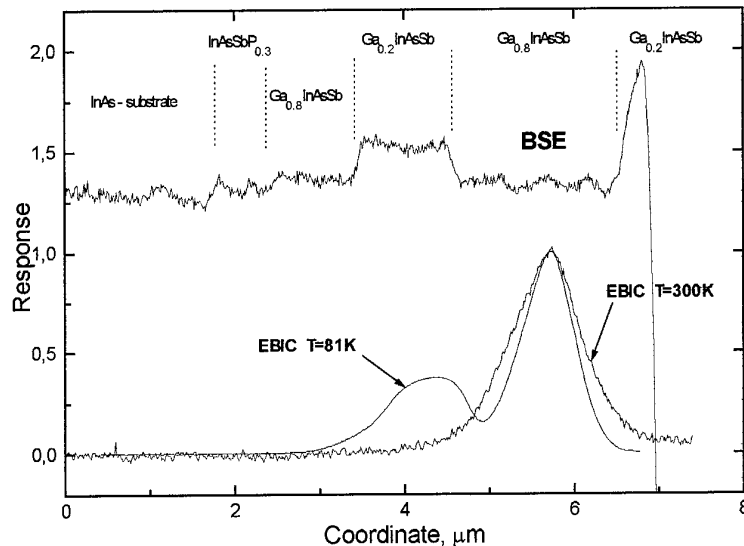


Figure 2 BSE and EBIC line profiles at $T = 81\text{K}$ and 300K for $\text{Ga}_{0.8}\text{InAsSb}/\text{Ga}_{0.2}\text{InAsSb}/\text{InAs}$ structure. Acceleration voltage - 10 kV.

Fig.1 demonstrated backscattering electrons and electron beam induced current line profile at $T = 81$ and 300K for $\text{InAsSbP}/\text{InAsSb}$ laser structure. Our study shows that by application of EBIC method we can obtain information about recombination activity of heterointerfaces.

So, Fig.2 demonstrates side by side with peak caused by p-n junction an additional peak in the region of $\text{Ga}_{0.2}\text{InAsSb}-\text{Ga}_{0.8}\text{InAsSb}$ heterojunction. This method application allows to determine what heterointerface is responsible for intersubband emission in type II fifth-layers laser structure.

4.3. Suppression of Auger recombination in the diode lasers based on type II $\text{InAsSb}/\text{InAsSbP}$ heterojunctions.

This section is devoted to overcoming Auger-recombination problem in $\text{InAsSb}/\text{InAsSbP}$ lasers with using type II heterostructures.

4.3.1. Theoretical consideration

Recently a theoretical study of radiative and non-radiative processes on type II heterointerface have been performed by G.Zegrya [24,25]. Type II heterojunction have the following main features:

- (i) valence band and conduction band offsets have the same signs (Fig.3),

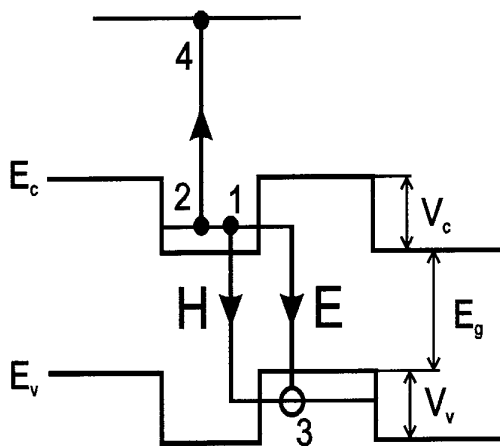


Figure 3 Schematic band diagram of type II heterostructure with quantum wells. The numbers 1 and 2 denote initial states of the particles, 3 and 4 denote the final states; H and E - two possible recombination channels of electron 1 and hole 3.

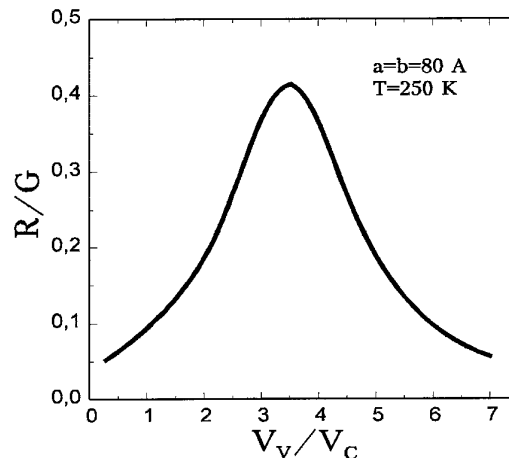


Figure 4 Radiative (R) and non-radiative (G) recombination rates ratio versus V_v/V_c relation. V_v , V_c are barrier heights in the conduction and valence band on the interface, respectively. Calculation performed for square quantum well $a=b=80\text{Å}$.

(ii) in contrast with the type I heterojunction, electrons and holes are separated in space, so that their recombination becomes possible only when carriers tunnel through the heterobarrier.

In type II heterojunctions two Auger-recombination processes are important: (i) Auger-process with participation of an electron and a hole with a transition of another hole to the spin-orbit splitting valence band (CHHS process) and (ii) CHCC process, with hot electron that transfer to conduction band, if $(E_g - \Delta)/E_g > m_c/m_{so}$, where Δ is the spin-orbit splitting energy, E_g is the effective band gap (See Fig.3) and m_c and m_{so} are effective electron mass and hole mass in the spin-orbit splitting valence band, respectively. As it was shown in [24], contributions to the Auger transition matrix element M from these other channels are of the same due to mutual transformation of light and heavy holes when they interact with the heteroboundary. These contributions to M have opposite signs and compensate each other when being summed. As a result, matrix element of the Auger-recombination process in type II heterojunctions has an additional infinitesimal of the order $[T_{mh}/(V_c m_c)]^{3/2} < 1$. Hence, the two channels of electron-hole recombination at the interface interfere destructively, which results to decrease of the matrix element and the Auger-recombination rate in type II heterostructures, but radiative recombination rates in type I and II heterojunctions are compatible, and their ratio is

$$R_{II}/R_I \equiv [T_{mh}/(V_c m_c)]^2 \leq 1.$$

Theoretical calculation performed for square quantum wells (See Fig.3) shows, that ratio between the radiative recombination rate R_{II} and non-radiative

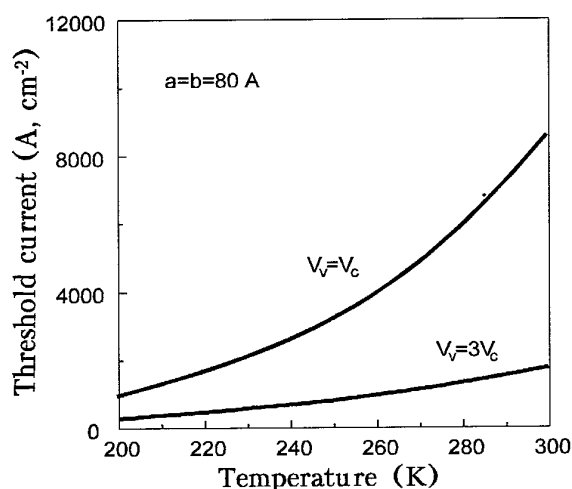


Figure 5 Calculated threshold current density temperature dependence for two values of V_V/V_C ratio.

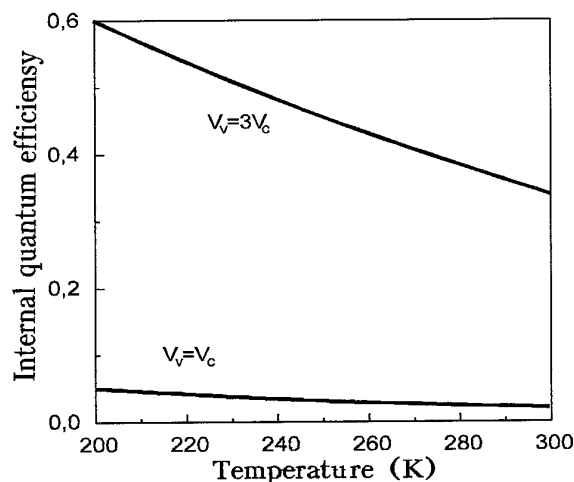


Figure 6 Calculated internal quantum efficiency versus temperature for two values of V_V/V_C .

recombination rate G_{AIL} , has a sharp maximum, that depends on ratio of barrier heights (or band offsets), V_V and V_C , in the valence and conduction bands respectively (Fig.4). So, we can suppress Auger-recombination rate by changing some parameters of the type II heterostructure. Fig.5 and Fig.6 represent also theoretically calculated curves for internal quantum efficiency and threshold current density versus temperature for laser structures with various band offsets ratio V_V/V_C . As one can see their values also depends strongly from band offsets ratio. There we would like to demonstrate it on the example of InAs(InAsSb)/InAsSbP heterostructures with type I and type II heterojunctions between active and confinement layers.

4.3.2. Experimental methods.

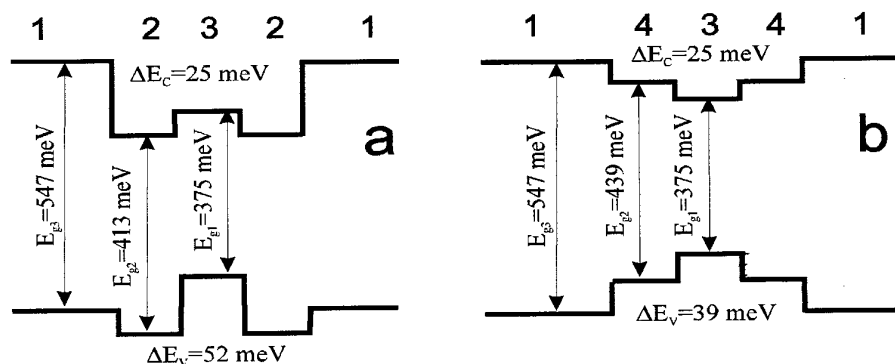


Figure 7 InAsSb/InAsSbP laser structures under study. a - type II heterojunction at the interface, b - type I heterojunction at the interface. Numbers denote the following layers: 1- InAs_{0.52}Sb_{0.18}P_{0.3}, 2- InAs, 3- InAs_{0.95}Sb_{0.05}, 4- InAs_{0.84}Sb_{0.06}P_{0.1}.

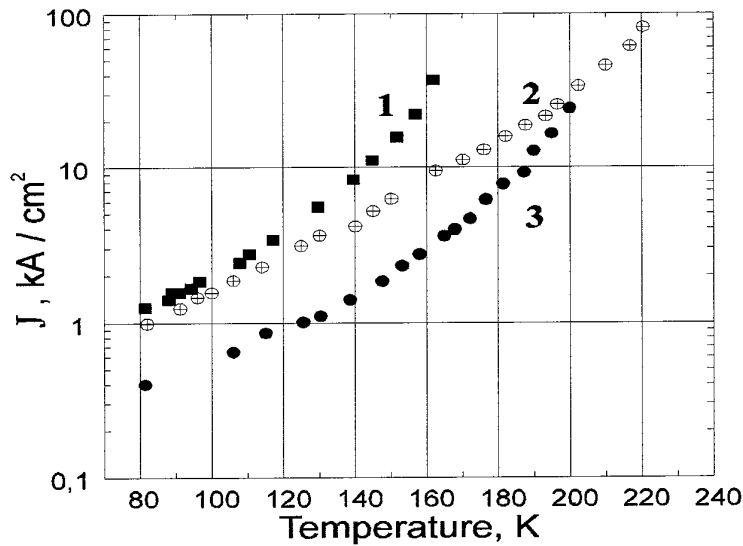


Figure 8 Temperature dependence of threshold current density for three set lasers grown by LPE

1-type I InAsSb/ InGaAsSbP laser, $T_0=25\text{K}$,

2-type II staggered alignment InAsSb/InAsSbP laser, $T_0=40\text{K}$,

3-type II broken-gap p-n GaInAsSb/InGaAsSb laser $T_0=47\text{K}$,

Two sets of InAsSb/InAsSbP laser heterostructures with separated electron and optical confinement were grown by LPE on InAs(100) substrates (See Fig.7). One of them (Fig.7 a) has a type II heterojunction with staggered alignment at the interface of active layer with a confinement layer and other structure (Fig.7 b) has type I heterojunction at the interface. In the first case the electron confinement was provided by InAs and in the second case electron confinement was grown from $\text{InAs}_{0.84}\text{Sb}_{0.06}\text{P}_{0.1}$. Active layers and optical confinement layers were the same for both laser structures, $\text{InAs}_{0.95}\text{Sb}_{0.05}$ and $\text{InAs}_{0.5}\text{Sb}_{0.16}\text{P}_{0.34}$, respectively. Band offsets in the conduction and valence bands, ΔE_C , ΔE_V , between active and electron confinement layers in DH lasers were nearly equal to $\Delta E_C=50\text{ meV}$, $\Delta E_V=39\text{ meV}$. In the lasers with separate electron and optical confinement, they were $\Delta E_C=15\text{ meV}$ and $\Delta E_V=52\text{ meV}$, so their ratio was about $\Delta E_V/\Delta E_C \approx 3.4$. Mesa-stripe lasers were fabricated by standard photolithography with stripe width of 15-55 μm and cavity length of 255-350 μm .

4.3.3. Results and discussion

We stated a task to study a suppression of Auger-recombination rate in laser heterostructures with various $\Delta E_V/\Delta E_C$ ratio. Some theoretical considerations were discussed above. It was shown in [24] that at ratio $\Delta E_V/\Delta E_C \approx 3\div 4$ a maximum suppression of the non-radiative recombination can be achieved (See Fig.7, where

the barrier heights at the interface V_C and V_V are equivalent to ΔE_V and ΔE_C). Besides increasing ΔE_V value affects positively on the hole localization in the active region of laser structure that is especially important for lasing achievement at room temperature.

The threshold current temperature characteristics (Fig.8) and differential quantum efficiency η (Fig.9) were studied for both types of InAsSb/InAsSbP laser structures, which were described in Sec.3, in depending on the temperature. It is important to emphasize that absolute values of threshold currents J_{th} , and quantum efficiency η , were similar for both types of the laser structures at $T=77K$, but temperature dependence of J_{th} and η differ strongly. If for type II InAsSb/InAsSbP laser the characteristic temperature was $T_0=35-40 K$ and limit operation temperature achieved $T_{max}\approx 220 K$ (curve 2 Fig.8), for the laser structure based on type I heterojunction $T_0=25-28K$, and limiting operation temperature was only $T\approx 145 K$ (curve 3 Fig.8). Essential difference was observed also in temperature dependence of differential quantum efficiency (Fig.9). If for both laser structures $\eta\approx 20\%$ at $T=77K$, it reduced to one-fifth by temperature decreasing from 77 up to 120K. Unfortunately not high enough values of band offsets on the interface with the active layer at room temperature do not allow to increase further operation temperature.

In such a way, a comparison of two types of laser structures with various

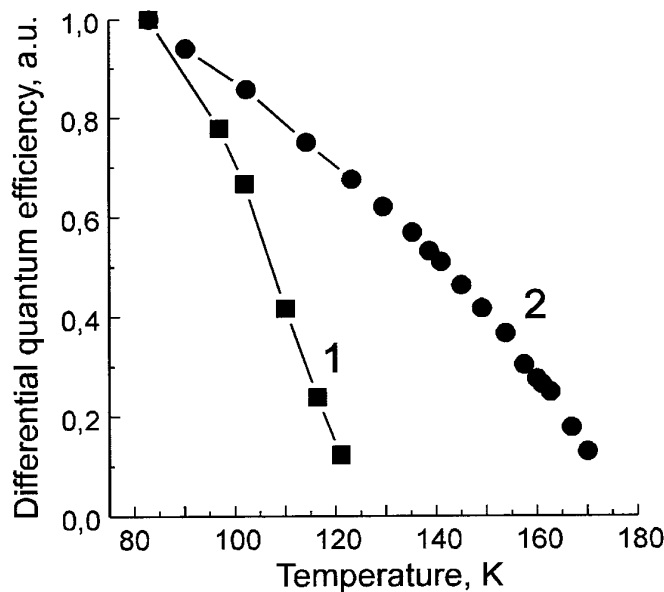


Figure 9 Temperature dependence of differential quantum efficiency η for two InAsSb/InAsSbP laser structure under study: 1- type II heterostructure, 2- type I heterostructure

$\Delta E_V/\Delta E_C$ ratio shows an essential improving temperature dependence of threshold current and a possibility to achieve higher operation temperature in laser structures based on lasers with type II heterojunctions at the heteroboundary with confined layer and higher value of $\Delta E_V/\Delta E_C\approx 3$. This experimental fact is the first direct confirmation of Auger-recombination suppression mechanism in type II heterojunctions with high values of $\Delta E_V/\Delta E_C$

ratio⁴. To compare affect of type I and type II heteroboundary on coherent emission, light polarization was studied. It occurred that both type of laser structure under study had a high contribution of TM-polarization (E is perpendicular to p-n junction plane). Polarization extent, α , was calculated by formula: $\alpha = (P_{TM} - P_{TE}) / (P_{TM} + P_{TE})$, where P_{TM} , P_{TE} are emission intensity for TM- and TE- polarized light. Maximum values of α were 80% and 73% (at current $J \approx 1.5 J_{th}$) for type II and type I heterostructures, respectively. TM-polarization characterizes indirect radiative transitions connected with interface-carrier interaction. So, we can conclude that in our InAsSbP lasers with type II heteroboundary between active and confined layers, interface radiative recombination prevails at the temperatures of 77-120 K.

5. CW high-power InAsSb/InAs/InAsSbP diode lasers for 3.4–3.6 μm spectral range

5.1. Experimental methods

The investigated lasers were InAsSb/InAsSbP double heterostructures (DH) grown lattice-matched to an InAs (100) substrata. The heterostructures were fabricated by liquid-phase epitaxy (LPE). They consist of a 0.5–1.5 μm thick active layer which is enclosed between two 3 μm thick InAsSbP cladding layers, (the calculated band gap energy E_g is 550 meV). The cap was 0.8 μm thick InAs layer. The composition of the active layer corresponds to lasing between 3.1 and 3.8 μm wavelengths. The carrier concentration in the nominally undoped active layer was about $4 \times 10^{16} \text{ cm}^{-3}$. The Sn doped n-InAsSbP confining layer had electron concentration up to $(2-5) \times 10^{18} \text{ cm}^{-3}$. The p-type confining and cap layers were doped with Zn up to 10^{18} cm^{-3} . Conventional photolithography and wet chemical etching processes were used to fabricate double channel chips were specially designed to be mesa-stripe geometry. It should be noted that the mesa is a very critical factor for obtaining a powerful single mode emission. On the one hand, an increase of the active area volume is desirable to obtain higher output power. A broad active region supports the generation of higher transversal/lateral modes. Previous tests show that single longitudinal mode lasing was observed when the stripe width not exceed 12 μm . Therefore the mesa and the channel width are 10 μm and 20 μm , respectively. The mesas were formed to have the depth of 7 μm . The InAs substrate was thinned and lapped to a thickness of 100 μm . Ohmic contacts were obtained by thermal vacuum evaporation of AuZn/Au and AuTe/Au on p- and n-side, respectively with following thermal annealing. The wafers were cleaved. The

cavity length were between 250 and 400 μm . The laser with uncoated facets is mounted by solder onto a copper heatsink that allows to install the laser into standard optical dewars (the Laser Photonics type).

The laser samples are mounted in a LN_2 -cooled Dewar working in the range of heat sink temperatures between 78 and 130 K. The stabilization of the heatsink temperature performed with an accuracy better than 100 mK. An 90° off-axis parabolic mirror (OAP) with 25 mm diameter is used to collimate the laser output beam. Reflective optics are used and aligned to minimize back reflections into the laser cavity. Electronically calibrated power meter measures the output power with 1 % absolute accuracy. A 1/2-meter Czerny-Turner monochromator and a HgCdTe-detector combined with a lock-in amplifier are used for recording the longitudinal mode structure. The high dynamic range of the data acquisition system (about 5 orders of magnitude) allows to identify all practically important weak side modes. A 4 cm long Germanium Fabry-Perot Standard are used to calibrate the tuning rate. Their finesses is 3.0, and their free spectral ranges (FSR) is 930 MHz. The laser far-field pattern is visualized by a pyroelectric video camera placed directly in front of the laser facet at the distance of 30 mm.

5.2. Basic electrical characteristics of lasers

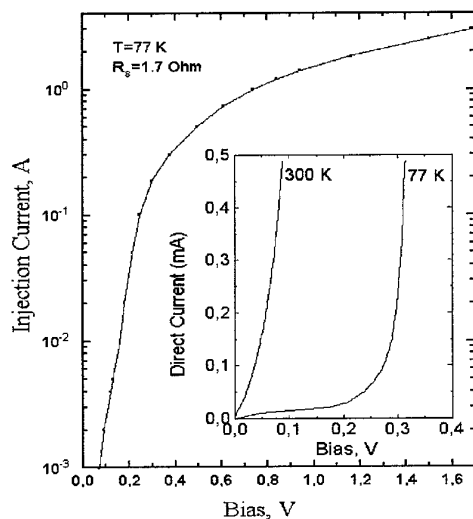


Figure 10 The current versus voltage of the InAsSb CW laser. For low and high direct currents the characteristics shown separately.

A current versus voltage curve measured both at 77 K and 300 K for 10 μm -width and 300 μm -length mesa laser is presented in Fig.10. The direct turn-on voltage and the series resistance of the laser are typically 0.23-0.4 V and 0.5 Ohm, respectively. The forward bias part shows close to exponential increasing with direct current. The saturated current I_s is about 1 mA if drive current derived from well known formula $I = I_s \cdot \exp(-E_g/kT) \cdot (\exp(eV/2kT) - 1)$. The laser can be driven without damaging of contacts up to 300-400 mA DC at cryogenic temperatures. It should be note that the best results could be achieved if the laser heatsink temperature has been stabilized before switch on a laser. At room temperatures it is better to limit the current by 20 mA DC. Taking into account

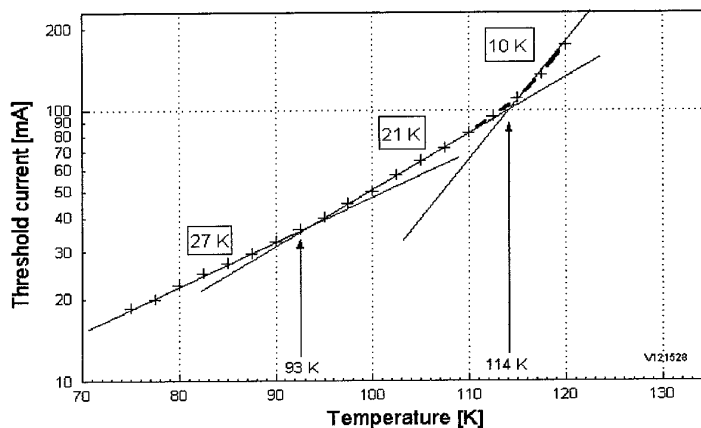


Figure 11 Temperature dependence of threshold current of the InAsSb CW laser in semi-logarithmic scale: experimental data and fit lines. Variations of the fit bow are observed at 93 and 113 K. The dash, dot and short dash-dot lines meet of three regions with different characteristic temperatures where different non-radiative processes are prevailed.

the voltage on the interfaces and the serial resistance this value is close to the band gap energy of the active layer.

5.3. Threshold current characteristics of the lasers

The laser has been tested up to 300-350 mA DC within a temperature range of 77 - 130 K. This region was determined by the good thermal contact the laser heatsink-cold reservoir inside the dewar and the power limit of temperature heater controller. However, for practical applications the temperature region close to LN₂ is important only. To obtain the lasing in 3 μm range InAsSb lasers are excited by DC higher than 2-90 mA at 80 K. The threshold current density is typically 600-800 A/cm². The threshold current I_{th} increases up to 180 mA with the temperature at 120 K as shown in Fig. 11. The threshold current dependence versus temperature is close to exponential. The characteristic temperature T_0 can be derived from: $I_{th} = I_{th}^0 \exp(T/T_0)$, where T is the heatsink temperature. It is decreased from 27 to 10 K with increasing of the heatsink temperature. Bow regions are in vicinity of 93-95 and 113-115 K. The experimental data agree to exponential fit with characteristic temperature $T_0 = 27$ K below 93 K. It is slowly decreased to 21 K above 95 K and fallen down to 10 K above 115 K. Normal diodes for spectroscopic applications show temperature limit of CW lasing at 90-97 K or 120-122 K. Last value is very

attractive for applications because allows to use these lasers inside a closed cycle dewars operated normally above 100 K.

Main factors influence on the temperature dependence of threshold current in InAsSb lasers as common for the III-V long-wavelength lasers could be determined by following main recombination processes: radiative recombination, non-radiative Auger-recombination, free carrier absorption and carrier leakage via interfaces with the active area. Results of the simple calculation of threshold current show that at low temperatures ($T < 93-95$ K) radiative recombination process prevails (the temperature dependence $I_{th} \sim T^{3/2}$) and contributes threshold current. Above this region ($T > 93-95$ K) the characteristic temperature slightly decreased by non-radiative CCHC Auger recombination (recombination of carriers passed to high-energy electron in the conduction band). This process has a temperature dependence as $I_{th}^{CHCC} \sim T^4 \exp(-E_g/T)$. Catastrophic increasing of the threshold above 115 K is evidence of strong carrier leakage via interfaces with the active area. The interface offsets to the confined layers prove on temperature dependence at higher temperatures. A high direct current overheating the active layer caused increasing of real temperature at high level of injection. This is very important process at higher temperatures when temperature increasing of the threshold ought to strong pump of the narrow bandgap diode laser with 100% duty cycle even at the threshold. Strong carrier leakage leads to suppression of CW lasing above 122 K.

5.4. Power-current characteristics

The total optical output characteristics of high power multi-mode laser at different temperatures are shown in Fig. 12 versus direct current.

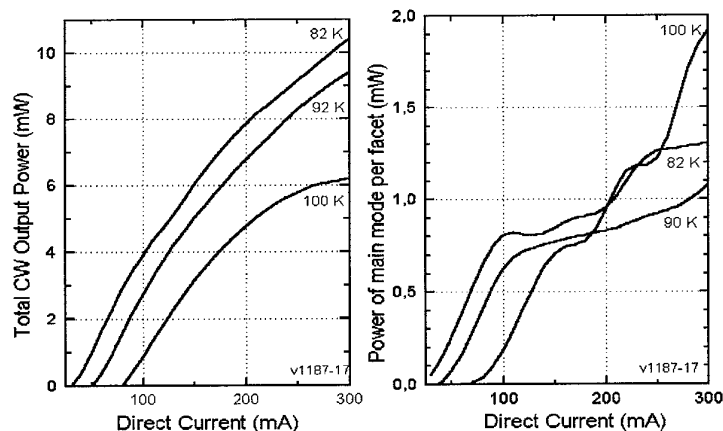


Figure 12 Optical output versus direct current of high power multimode laser (left). The small saturation becomes under high dc above 100 K. Distribution of optical power over lasing current of multimode InAsSb CW laser (right).

different temperatures are shown in Fig. 12 versus direct current. No significant variations of output characteristics observed below 93-95 K. The power begins to saturate at 3.6 times above the threshold current (I_{th}) at 100 K. The external efficiency at 82 K was 0.078 W/A near threshold. Its decreasing down to 0.028 W/A at 8 times above the threshold can be

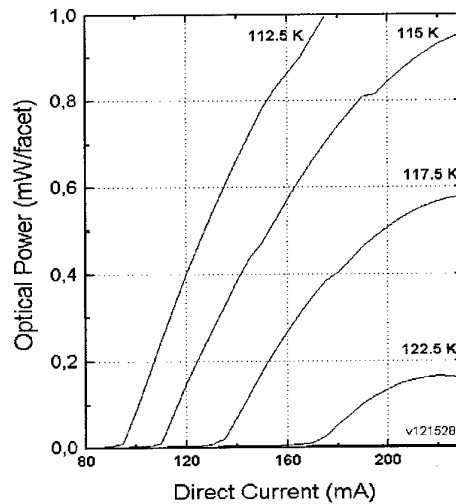


Figure 13 Output power characteristics of InAsSb CW laser above 105 K temperature.

caused by junction overheating.

The internal loss, α_{int} , has been calculated from the dependence of the output power on the drive current [23]:

$$P_{\text{out}} = \frac{h\nu}{2e} \alpha_m / (\alpha_m + \alpha_{\text{int}}) * (I - I_{\text{th}} - \Delta I_L),$$

where P_{out} is total optical power, $h\nu$ is the photon energy, e is electron charge, ΔI_L is temperature increase of the leakage current, $\alpha_m = 1/2L * \ln(1/R_1 R_2)$ is the external optical loss, α_{int} is the sum of the cavity's internal losses (including optical losses in the active area, in the confinement, in interfaces, due to carrier diffusion and non-radiative recombination), L is cavity length, R_1 and R_2 are the facet reflectivity. For our experimental conditions with typical reflectivity of 31% α_m equals to 40 cm^{-1} . Assuming that up to 100 K the temperature increase of the leakage current is small we can calculate that α_{int} is close to $20\text{-}25 \text{ cm}^{-1}$. It should be pointed out that it is very small in comparison to the typical value [24] for InAs diodes of 40 cm^{-1} . Up to 11 mW CW power has been achieved from such LPE-grown lasers with reduced losses in the laser cavity. The dependence of CW output power on injection current and heatsink temperature above 105 K is pointed out in Fig.13. The power for this region was limited by value of to 1.0 mW at temperatures above 113 K. At higher temperatures it begins to saturate due to strong gain reduce by leakage. Therefore these lasers could be better applied up to the temperatures of 115-117 K. For spectroscopic applications a power of single frequency mode is only important relative to total output one which is dispersed over the number of lasing

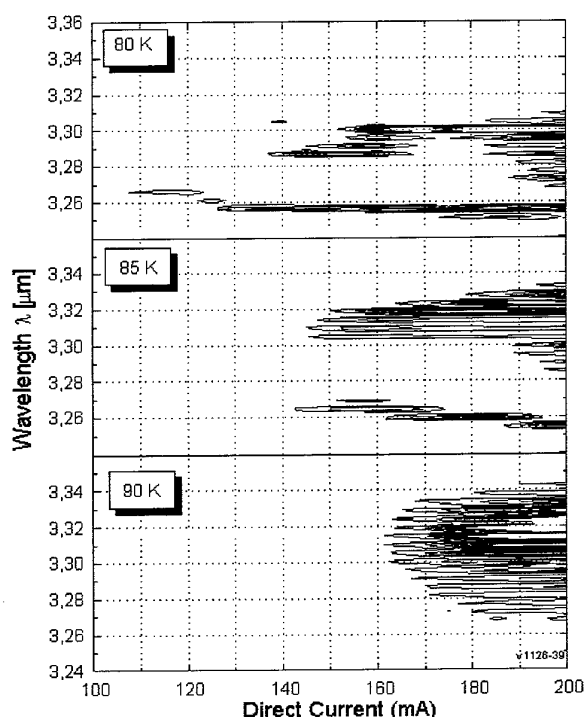


Figure 14 Mode maps as a top view of 3-D spectra plot of lasing of the multi-mode InAsSb CW laser. In the mode map the black color follows to higher optical power, white is close to the level of background radiation. The upper plot - $T = 80$ K. The bottom plot - 95 K.

the same spectral position. At low currents the lasing spectra consist of 4-5 homogeneously distributed modes with a mode spacing of 5.4 cm^{-1} . At currents higher than 280 mA the amount of excited modes is reduced. The mode spacing becomes twice relative to normal operation.

The CW output power of single-mode laser is limited by 2 mW with a weak temperature dependence below 93-95 K.

5.5 Multi-mode and single-mode InAsSb lasers

Multi-mode lasers

Consider the spectral features of multi-mode InAsSb CW lasers. Mode maps (a top view on a 3-D spectra) of lasing shown in Fig.14 for three different temperatures. At low temperatures it is shown a presence of large energy "hole" in

wavelengths. The distribution of the power over lasing modes for different heatsink temperatures was investigated. For multi-mode laser single frequency oscillations were observed only in the vicinity of the threshold (up to $1.1 I_{th}$) where the mode spectra envelopes were narrow. However for this range the single mode power was not sufficient (as low as 0.1 mW). A small electron density can not generate a sufficient number of photons. Under higher injection 4-6 lasing modes were observed. The total optical power is distributed among all lasing modes. The mode power is limited by 1.3 - 1.4 mW. Highest values of mode power are achieved under higher currents and at low temperatures as for conventional diode lasers.

At higher temperatures (over 100 K) the main mode power increases decreasing number of lasing modes. The power saturation is observed at the

lasing modes. Nevertheless our test of laser far-field pattern has shown that lasing occurs on the main spatial mode (see Fig.15). Highest spatial modes are suppressed.

At 80 K the lasing spectrum consists only of single mode up to 1.4 times above the threshold. The mode spacing was 4.3 cm^{-1} that corresponds to effective refractive index of 3.58. The output power is slightly increased with drive current. It should be note that output power characteristic of the laser is increased with current without sharp leaps and downfalls. But the mode jumps to abnormal (for III-V semiconductor lasers) short-wavelength side. After jump the main mode is stabilized and live over wide current range up to two times of threshold. Next longer wavelength side mode is excited at $1.4I_{th}$ and consequently tunes and jumps via neighboring modes towards normal long wavelengths. At higher pumping level the lasing is excited on side modes, with wide hole in lasing spectra as high as 6-mode spacing being occurred. Inside the hole no lasing modes are observed. Increasing of injection current up to one in 1.8 times above the threshold leads to excitation of intermediate spectral modes and filling of the hole in the lasing spectrum. The longer wavelength mode becomes prevailed.

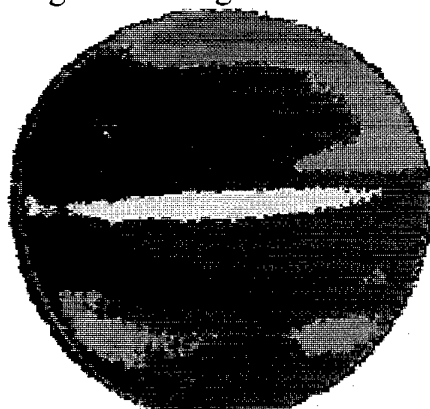


Figure 15 Far-field pattern of multi-mode InAsSb CW laser as it was visualized by pyroelectric videocamera. The distance between the videocamera and the laser facet was 30 mm.

This feature of lasing occurs at higher temperatures too. The temperature rising to 85 K causes to excitation both groups of modes simultaneously just at the threshold. The hole in the spectrum is increased up to 8-mode spacing where lasing mode are suppressed. The main lasing mode tunes by DC towards longer wavelengths. However already at currents in 1.1 times above the threshold the spectrum becomes asymmetrical, with the long wavelength mode being dominate. With future current rise, mode from longer wavelength group is amplified and short wavelength mode becomes tune to shorter wavelengths. Under current of $1.3 I_{th}$ the spectral position of main long-wavelength mode becomes stable. Short- and long-wavelength side modes are excited around it to make symmetrical

gain spectrum. These modes fill the spectral hole in lasing. After excitation of side mode a big mode jump is not occurred.

With future increasing of temperature up to 90 K, it is shown normal excitation of multi-mode lasing with homogeneous broadening of the emission spectrum. Therefore features of InAsSb multi-mode laser can be explained by inhomogeneous of gain spectrum. At low temperatures and small injection current the gain spectra are homogeneous broadened. In vicinity of the threshold the gain

small exceeds losses, and the lasing occurs only at main longitudinal mode. The increasing of free carrier absorption and variation of effective refractive index under increasing of carrier concentration, leads to abnormal short-wavelength tuning of lasing wavelength by direct drive current in the InAsSb lasers even above the threshold. With future increasing of current and carrier concentration the gain spectrum is deformed. The lasing at 6-9 long-wavelength modes are suppressed. Future rising of injection current with 100 % duty cycle as well as heatsink temperature (to 90 K) cause to homogeneous thermal broadening of gain spectrum and increasing non-radiative recombination (CHCC Auger and carrier leakage via small band offset interfaces). The observed hole in the gain spectrum is caused by long carrier intraband relaxation that can be rough estimated as $\tau=2h/\Delta E=45$ ps.

Single-mode lasers

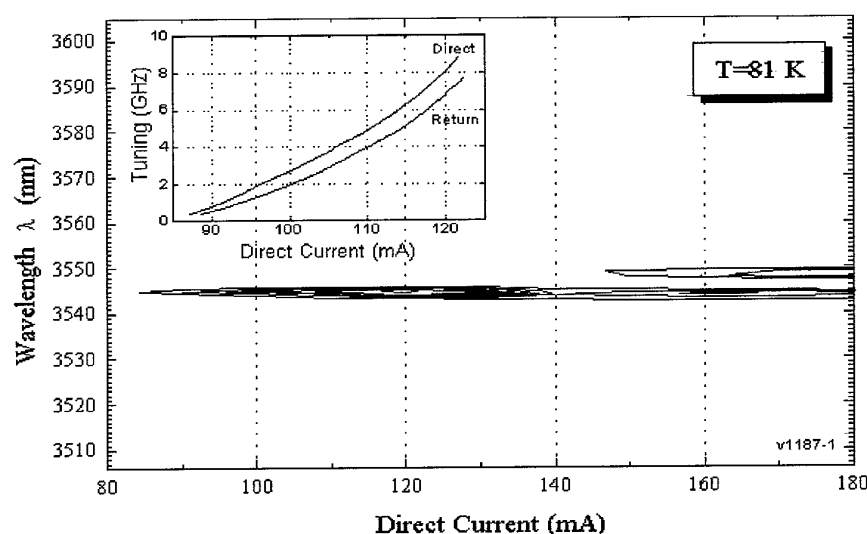


Figure 16 Mode maps and far-field patterns of lasing of the single-mode InAsSb laser at 81 K. Inset demonstrates the tuning rate versus direct current dependence for increasing and decreasing of current.

The spectrum of single mode laser that was recorded at 81 K is depicted as the example in Fig.16. The laser is operating at the fundamental longitudinal mode with a beam divergence of 30*50 degrees. The mode spacing for this laser is 3.9 cm^{-1} . The lasers have the spectral characteristics that are common to a Fabry-Perot free-running diode laser. The single frequency oscillations are observed above the threshold I_{th} only up to $1.7 \cdot I_{th}$. The mode suppression ratio (MSR) is up to 18 dB.

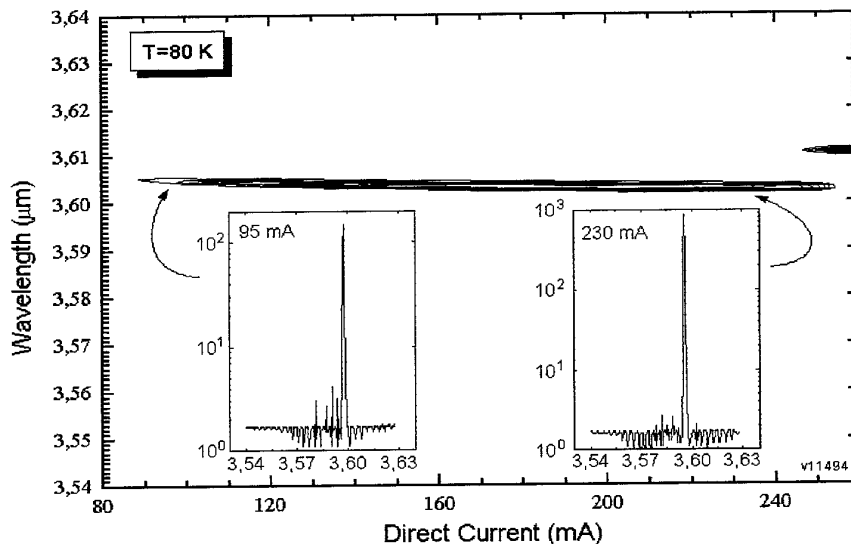


Figure 17 Mode maps of lasing of the single-mode InAsSb CW laser with high mode suppression ratio at 80 K. Insets demonstrate suppression of side modes. Highest value of MSR as high as 27 dB has been achieved for Fabry-Perot free-running laser in the mid-infrared. Direct tuning by current is to shorter wavelengths, mode jumps to longer wavelengths.

Two regions of different features of lasing spectra should be mentioned: 90-93 K and 110-115 K. Inside the each temperature region the mode plots are similar. Below 90 K these lasers have a single mode operation region up to 2-2.5 times above the threshold. Each lasing mode lives during increasing injection current on 10-15 mA DC and then jump to next mode towards to longer wavelengths. At higher injection current it is excited 8-10 modes on the single mode spacing distance, with shorter wavelength mode being dominated.

Increasing heatsink temperature above 90 K leads to extension the region of quasi-singe mode lasing and to simultaneously lasing at two modes separated by 8-10 mode spacing distance. When the temperature is increasing above 100-115 K mode lives about 20-30 mA and jump to long wavelength side mode. At whole temperature range the laser wavelength tuned by direct current towards shorter wavelengths, but the mode jump took place to the next side mode at the long-wavelength side. The DC tuning rate decreases between 1.5 GHz/mA and 600 MHz/mA with temperature rising from 82 K to 93K. The rate falls down to 70-100 MHz/mA above 110 K. At given temperatures the tuning rate is reduced with DC increasing (from 1500 MHz/mA to 970 MHz/mA and then to 270 MHz/mA under current rise from 40 to 200 mA). The amplitude/frequency modulation index was about 9.9 nW/MHz at 81 K and decreased down to 5.8 nW/MHz at 90 K. The

continuous tunable covering spectral range without mode hopping (CTSR) is 21-24 GHz which was 18-21% of the mode spacing. The temperature-tuning rate was 400 MHz/K below 85 K and about 1.9 GHz/K above. It should be mentioned that the mode lives during a very wide temperature interval of more than 10 K and continuously tunes by temperature over 14 GHz (12% of the mode spacing) without mode jumps towards the shorter wavelengths too.

Interesting features shown single mode lasers with highest MSR that spectra are presented in Fig.17. Single frequency region of lasing between the threshold and nine times above it was obtained from these devices. For free running conventional Fabry-Perot diodes this region of single frequency lasing is really very broad. With temperature rising this region was reduced by the range of available injection current (with increasing of the threshold on temperature and keep the same of upper limit of injection current for given diode). However the single frequency lasing has been kept over all temperatures. The MSR is as high as 27 dB is achieved. Typically the mode jumps to the long wavelength side through 2-5 neighbor modes. The mode spacing was $4.5\text{-}5.5\text{ cm}^{-1}$. The mode operates over a wide current range again. Weak side modes (MSR of about 15 dB) can be found with a distance of several mode spacing only from shorter wavelengths. It should be noted that no weak side modes were found at the long-wavelength side.

5.6. Long term stability of 3.4 μm CW laser performance

Long-term stability of the laser wavelengths and output parameters under normal running conditions of a laser device inside a TDLAS spectrometer are investigated during a practical operation period of one year. CW lasers are running close to LN₂ heatsink temperatures ($T=85\text{-}95\text{ K}$) with an average output power of about 1 mW/facet. The lasers are mounted inside a Laser Photonics Dewar. As a part of a measurement program the selected diode was operating during a week then it was heated up to room temperature, and cooled down again to LN₂ before the next tests. The total time of operation can be roughly estimated to $(1\text{-}2)\cdot 10^3$ hours, with an injection current of about 2-3 times above the threshold. It should be pointed out that typical reasons for catastrophic collapses of InAsSb lasers were injection of very strong (up to 10-12 times above the threshold) DC. Relying on these tests it should be pointed out that a CW output power of 2 mW (about 10 MW/cm^2) did not destroy the uncoated laser facets. The maximal decrease in CW output power took place in the first half year of operation. After that the output power decreased by about 40%. During the next period the degradation of the output power was less than 20%. It should be noted that this maximal changing was observed when the injection current exceeded in 4-5 times the threshold one. Less

than 15 % power degradation was observed under injection current below $4I_{th}$. Stability of spectral characteristics of laser diodes is one of the most important requirements for application of a laser in a TDLAS spectrometer. The reproducibility of the lasing wavelength was periodically measured by recording laser mode maps. Dramatic variations in the laser spectra were not observed. It kept close to single frequency oscillation, with the main mode wavelength being at the same position during the whole test period with cycles of heating and cooling. The presented characteristics demonstrate a very important feature of fabricated laser relative to lead-salts ones: the position of the lasing mode is the same during a long period and a lot of cycles of cooling down to LN_2 and heating up to room temperature. We can explain this fact by good stability of the III-V semiconductors. Differences were observed only at current values where mode jumps happened, especially for weak side modes under high injection currents. The short-term lasing wavelength drift was measured to be as low as 0.4% over temporal interval of 20 min. The direction of the drift, which was observed, is to shorter wavelength side. Therefore these lasers are very promising to be used in TDLAS spectrometers.

To practical tests of the designed lasers to the spectroscopic applications in the wavelengths around 3 μm , the InAsSb lasers were put into a FM-TDLAS spectrometer equipped with a multi-reflection absorption cell for ambient measurements. Absorption band of formaldehyde at 2921.5 cm^{-1} was detected with the 3.4 μm laser. A detection limit of $5 \cdot 10^{-6}$ in terms of optical density was estimated. The minimum detectable concentration was 1 ppbv. The 3.6 μm laser observed the absorption of band at 2800.28 cm^{-1} . The laser is shown to be suitable for the detection of ambient HCHO-concentration levels of the world best level. During the work with InAsSb laser it was found that formaldehyde line strengths listed in HITRAN92 [1] were wrong and it was corrected according to our experiment.

7. Theoretical analysis of non-radiative losses in the longwavelength quantum well lasers (leakage current, Auger-recombination, intervalence band absorption, effect of heating).

First we consider theoretically main factors which limit operation temperature and threshold current in an active layer of longwavelength laser structure with quantum wells.

Main contributions in the total value of the threshold current are the following (See Fig.18):

- radiative recombination and appropriate current density is

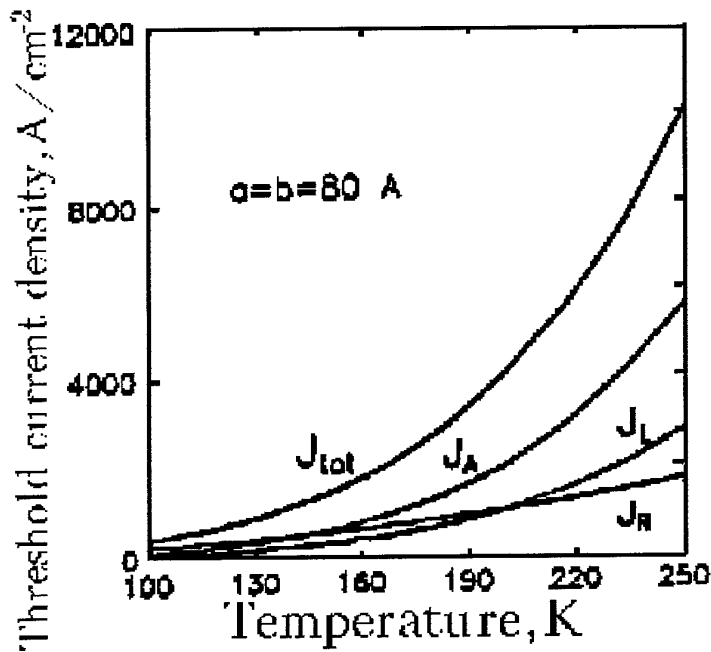


Figure 18 Theoretical calculation of threshold current density versus temperature for longwavelength laser structure with quantum well active region.

$$J_{thR} = e * R_R = e n_{th}^2,$$

where n_{th} is a concentration at the threshold of generation,

- Auger recombination and appropriate current density

$$J_{thA} = e * G = e C_A n_{th}^3,$$

- a process of current leakage from quantum well due to Auger-recombination (See Fig.18) and appropriate current density is J_{thL}

The rates of all above processes depend on temperature according as power law.

At $T > 150K$ temperature dependence of

the threshold current is non-linear:

$$n_{th} \sim T^\alpha,$$

where $1 < \alpha < 2$. Therefore Auger-recombination current is

$$J_{thA} = e C_A n_{th}^3 \sim T^{3\alpha},$$

at $T > 150K$ $\alpha \approx 5/3$. Then at high temperatures we have $J_{th} \sim T^5$. Our analysis shows that in the field of $T > 150K$ threshold current depends strongly on temperature, as T^5 . As it will be shown below our experimental results follow to this dependence. Such strong temperature dependence of J_{th} is due to abrupt temperature dependence of the threshold concentration n_{th} [25].

Theoretical calculation shows that in longwavelength quantum well lasers a significant intraband absorption due to free carriers takes place [25,28]. This fact influences strongly the condition at the coherent generation threshold. As a result threshold concentration n_{th} depends strongly (non-linear) on temperature (See Fig.19). Abrupt temperature dependence of n_{th} leads in turn to abrupt threshold current temperature dependence.

As it has been shown in [24], Auger recombination rates in the type-II and type-I heterostructures are different. Suppression of Auger recombination can be achieved in the type-II heterostructures under some circumstances.

As it has been reported in [25] in the type-II heterostructures the suppression of intraband absorption takes place also. It should be noted that these considerations open the way to improving internal quantum efficiency and increasing operating temperature of mid-infrared III-V semiconductor lasers.

The following important contribution to losses is an overheating in laser structures [27]. Under the Contract the analysis of overheating effect has been made. We investigate a process of overheating and consider the model of hot carrier relaxation in the mid-infrared double heterostructures that can operate at room temperature.

To study a role of carrier heating laser heterostructures with n-GaInAsSb active region were made. The GaInAsSb bandgap energy was 530 meV at room temperature, thickness of an active layer was 1.5 μm . The GaAlAsSb cladding layer had 1.27 eV bandgap and was of 2.5 μm thickness. The heterostructures with different values of band offsets on N-n heteroboundary were fabricated. It was

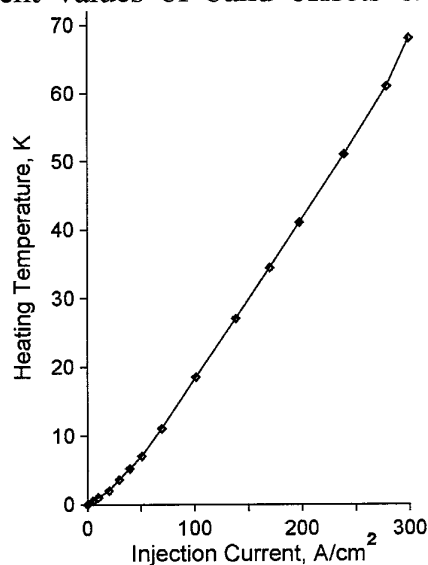


Figure 20 Heating of the active region for GaInAsSb/GaAlAsSb heterostructures. The heating temperature was defined as difference between effective temperature of electron-hole plasma under given current and heatsink temperature.

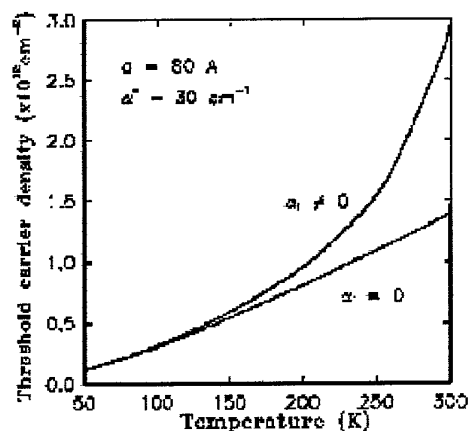


Figure 19 Threshold carrier density versus temperature with/or without taken into account intravalence band absorption

varied by grown of additional GaAlAsSb wide-gap layer and increased of GaInAsSb bandgap. All structures were grown by LPE.

The current-voltage and Watt-Ampere dependencies, luminescence spectra and carrier lifetimes versus amplitude and pulse duration of input injection current were studied under direct and short pulsed current. The voltage-temperature method described before in [27] was used for determination of the overheating. Fig.20 shows that the overheating increases up to $T_0=70$ K in the vicinity of the room temperature. It has different current dependence for the cases of small and strong injection. The overheating is also a function of the

band offsets. The optical output characteristics versus current has a power dependence, with the slope is $3/2$ under small current (up to 100 A/cm^2). The slope decreased down to $2/3$ with injection increasing.

The experimental results show that the overheating strongly influences on both threshold current density and output power of mid-infrared lasers in the vicinity of room temperature. The main processes leading to the heating in the active region are following:

- Overheating by hot carrier injection over the interface
- Overheating by Auger excitation of carriers
- Overheating by intraband absorption of stimulated emission.

All these mechanisms make a contribution to recombination at mid-infrared heterostructures. The overheating processes should be suppressed to increase operating temperature and improve threshold characteristics of longwavelength lasers. As well as suppressing of Auger recombination and intraband absorption, the corresponding overheating processes could be suppressed in the type-II heterostructures. Therefore only overheating due to carrier injection over the

interface should be main process limited operating temperature of type II laser structure.

The carrier life times for GaInAsSb lasers were calculated at room temperature (Fig.21). As the electron-electron interaction in GaInAsSb is faster process (curve 1, Fig.21), the considerable part of the excess energy of hot carriers is transported to the electron system.

The temperature of electrons in active layer T_e is higher than holes one which have the lattice temperature T_o . In the lattice there are two systems (phonon and electron) with different temperatures and $T_e > T_o$. The excess energy that has been transmitted to the electron gas can be transferred to the phonon system by electron-phonon collisions (curve 3, Fig.21) or disappeared into the ambient medium and adjacent GaAlAsSb emitter regions (curve 4, Fig.21).

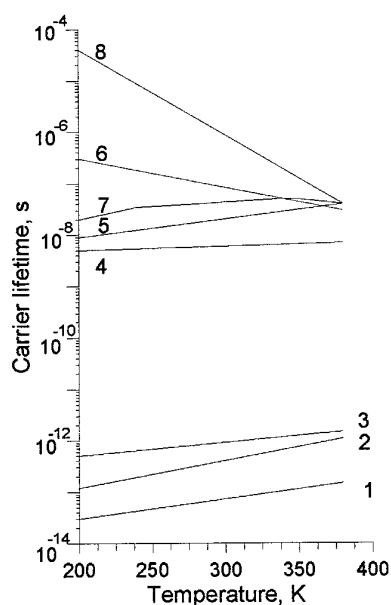


Figure 21 Calculated relaxation times vs. temperature: electron-electron (1), electron-hole (2), electron- LO-phonon (3) interactions, energy relaxation to ambient and emitters (4), phonon-electron (5), phonon-phonon (6) interactions, and CHCC-Auger (8) processes. Experimentally measured radiative recombination time (7).

We considered overall channels of the internal energy losses. Under small currents (up to 60 A/cm^2) only LO phonons interact with non-equilibrium heating electrons. The electron-phonon interaction can move the emission wavelength. When threshold current raises, all phonons interact with hot electrons. The lattice T_0 and the electron gas temperature T_e are increased (up to T_1). The electron and phonon systems have the same temperatures ($T_1 \sim T_0$).

It has been pointed out that the contribution into overheating of Auger-processes causes an additional heating of carriers up to 8-10 K. This value is more than calculated one for bulk Auger processes [28]. The lifetime relaxation for the emission τ_{exp} depends on the band offsets. Comparison τ_{exp} for the heterostructures with different bandgap values shown that $\tau_{\text{exp}} \sim f(E_G)$, but the theoretical data for radiative lifetime give $\tau_r \sim f(1/E_G)^7$. Comparing experimental τ_{exp} , calculated τ_r in depending on E_G and theoretical contribution of bulk Auger process rate we conclude that the recombination in vicinity of the interface strongly influences on the heating.

This process can be suppressed, for example, using smooth or graded interface that can be easily realized by LPE growing.

In conclusion we can predict that overheating processes due to Auger-excitation of carrier and intravalence band absorption can be suppressed in mid-infrared lasers based on type II heterostructures. Our study shown also that leakage currents in mid-infrared III-V semiconductor lasers could be decreased by utilizing the type II broken-gap heterojunction where bulk Auger recombination, and overheating could be suppressed.

8. Advanced type II broken-gap p-GaIn_{0.17}AsSb/n-In_{0.83}GaAsSb heterolaser.

During preceding work fulfilled in the frame of EOARD Contract F6170894C0011 1994/1995 [32] new physical approach have been proposed and a novel tunneling-injection mid-infrared laser employing a type II broken-gap p-p GaInAsSb/InAs heterojunction in active region have been designed and studied [30,31,33]. The main feature of this new laser device was the lasing provided by tunneling injection of electrons and their tunneling-assisted radiative recombination with holes at the heterointerface. Cladding layers from InAsSbP alloys were used in this laser structure. Such design allowed to suppress non-radiative Auger-recombination process at the interface, to relax a temperature dependence of the threshold current, and to increase characteristic temperature up to $T_0=40\text{-}60\text{K}$ in the range of 80-110K. The laser wavelength and threshold current density were

$\lambda=3.26 \mu\text{m}$ and 2 kA/cm^2 respectively at $T=77\text{K}$. Limit operating temperature in pulse mode $T\sim 125\text{K}$ was achieved [33].

But further improving laser performances was limited by hole leakage at the interface and high value of the threshold current. It induced us to search a new approach to laser structure design.

As a new approach we proposed to include type II broken-gap p-n heterojunction in an active region of the new laser structure to improve its temperature performance. Due to a difference in band energy diagrams of a type II p-p and p-n heterojunctions at applied bias we waited that in the case of p-n junction we can exclude or suppress hole leakage current from wide-gap semiconductor in the narrow-gap one which plays an important role in p-p broken-gap heterostructure and try to reduce a threshold current in new laser structures.

8.1 Electroluminescence in type II broken-gap p-n heterostructures.

For the first, we investigated electroluminescence in single p-n heterostructures.

Heterostructures were prepared by growing Zn-doped wide-gap quaternary p- $\text{Ga}_{0.83}\text{In}_{0.17}\text{As}_{0.72}\text{Sb}_{0.18}$ (carrier concentration was $4\cdot 10^{16} \text{ cm}^{-3}$) on n-InAs (100) substrate ($n=2\cdot 10^{16} \text{ cm}^{-3}$). Current-voltage characteristics and electroluminescence properties of these heterostructures were studied at forward and reverse applied bias.

Fig.22 represents band energy diagrams of type II broken-gap p-n GaInAsSb/InAs heterostructures under forward (a) and reverse (d) bias as well as electroluminescence spectra and current-voltage characteristic. Intensive emission was observed at both bias polarities at $T=77\text{K}$. Under forward bias ($V>0$) current-voltage characteristic was monotonous. Infrared electroluminescence occurred at $V\geq 0.4 \text{ V}$ (Fig.22 b). Emission spectra consisted of two bands, longwavelength band ($h\nu_1=333 \text{ meV}$) and shortwavelength one ($h\nu_2=392 \text{ meV}$). Maximum photon energy of $h\nu_2$ was close to $E_{g\text{InAs}}=408 \text{ meV}$, at $T=77\text{K}$, and we supposed that in this case radiative recombination appears in the bulk of n-InAs. The second wide band $h\nu_1=333 \text{ meV}$ can be due to recombination of electrons from well at InAs side with Auger holes at the different side of the heterointerface. Indeed, in the case of p-n broken-gap heterojunction (Fig.22 a) electron quantum well at the interface must wide enough, and there are many electron states in it, which form enough spreading band. Emission intensity of $h\nu_1$ band is much lower than $h\nu_2$ band.

Under reverse bias ($V<0$) the p-n heterostructure possessed S-shape I-V characteristics with a pronounced interval of negative differential resistance (NDR)

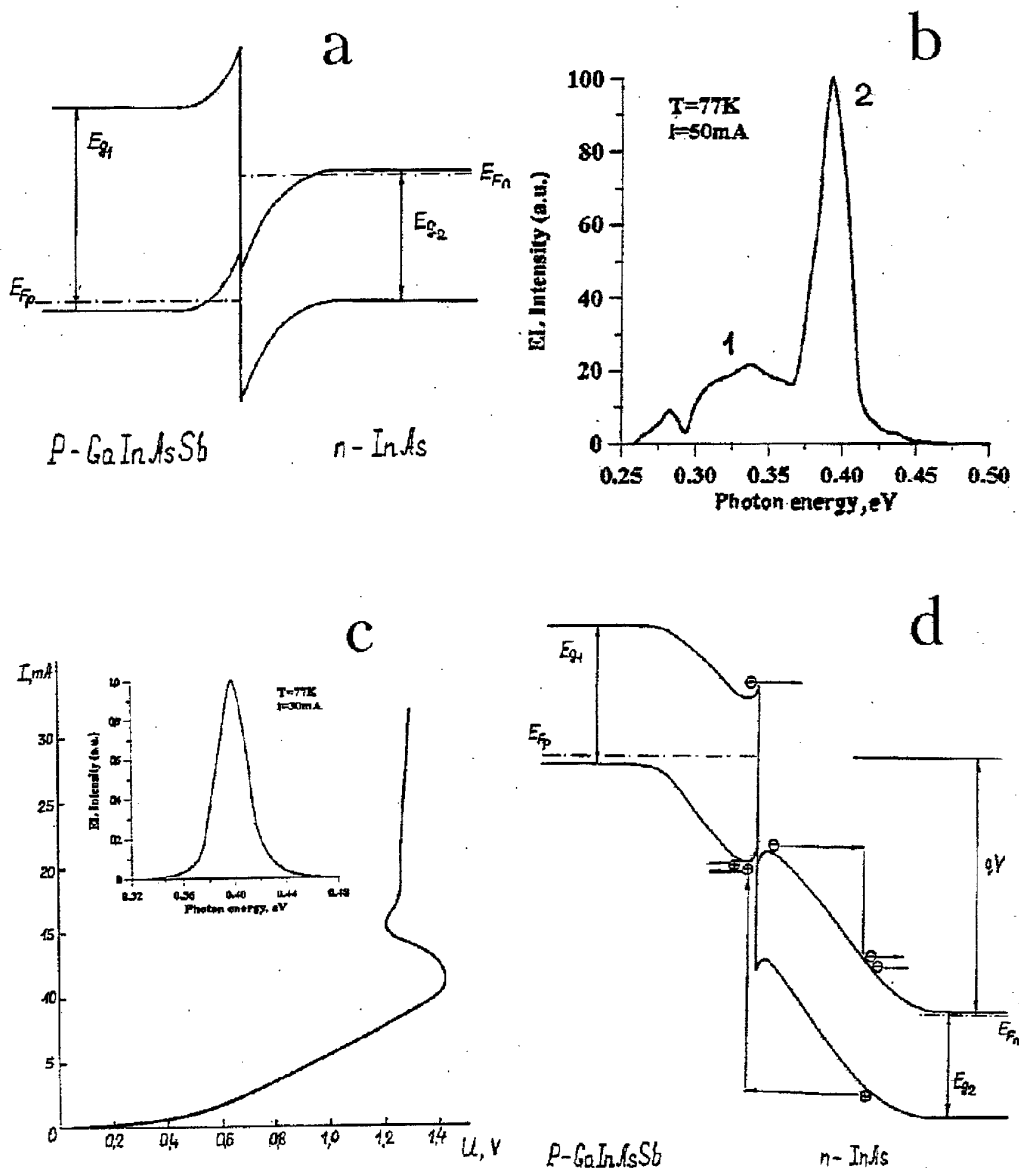


Figure 22 See text.

(See Fig.22 c). In this case electroluminescence with only one very intensive emission band ($h\nu=397$ meV) (See inset) sharply occurred after the current increasing above NDR range. This fact can be explained by consideration of an energy band diagram of the p-n broken-gap heterojunction under reverse bias (Fig.22 d).

The applied field extracts now both electrons and holes from the vicinity of heterojunction which leads to formation of double space charge region there.

Existence of a small gap at the interface initiates limited electron emission into bulk of n-InAs wherein their essential heating is getting possible. As the bias increases ($V \geq 0.5V$) the part of electrons gain their energy high enough for impact ionization in InAs ($E_i \approx 0.42\text{eV}$ at $T=77K$). Note that only 1 or 2 acts of impact ionization for given $V < 1.4V$ are potentially possible for the "cool" electrons emitted directly from the gap at the interface. But it is not sufficient for the development of the spatial avalanche breakdown in InAs.

To our opinion just evolution of avalanche breakdown with participation of impact ionization events at the both sides of the heterointerface are principal for realization of NDR. Such process can be initiated by those holes that are generated in the bulk of InAs and acquire energy $\sim 0.4\text{eV}$ near the heterointerface in the space charge region. When the hot holes occur in the wide-gap quaternary layer they have energy in order to $2E_{g2} \approx 0.82\text{ eV}$ (it is higher than $E_{g1} = 0.63\text{ eV}$). The existence of such hot holes near the heterointerface and their interaction with the heteroboundary, which allows to violate the momentum conservation law, leads to high probability of impact generation of electron-hole pairs. After this process the new electrons occur in n-InAs, and holes - in p- GaInAsSb layer. So, heteroboundary is an effective source of hot electrons in n-InAs. As a result a multiplication process becomes avalanche-like one. As far as the quantity of hot carriers increase with the current rising, conditions for evolution of avalanche breakdown according to a mechanism described above realize under lower reverse biases. It can explain NDR occurrence satisfactory. Existence of NDR leads to instability of the homogeneous current distribution, and hence to current filamentation. In the filament region non-equilibrium electron and hole concentrations sharply increase, and it produces a favorable conditions for intensive radiative recombination.

With taken into account results of the theoretical analysis and the electroluminescence experiments we have designed a new laser structure with type II broken-gap p-n heterojunction in an active region.

8.2. Tunneling-injection heterolaser with type II broken-gap p-n heterojunction

Tunneling-injection heterolaser with type II broken-gap p-n heterojunction in active layer was grown by LPE on p-InAs (100) substrate (Fig.23). Active layer was made by two quaternary layers of $\text{Ga}_{1-x}\text{In}_x\text{As}_y\text{Sb}_{1-y}$, wide-gap ($x=0.17$, $E_g=640\text{ meV}$) and narrow-gap ($x=0.83$, $E_g=326\text{ meV}$) which formed near broken-gap alignment at the interface. Additional InAsSbP layers were used to improve an

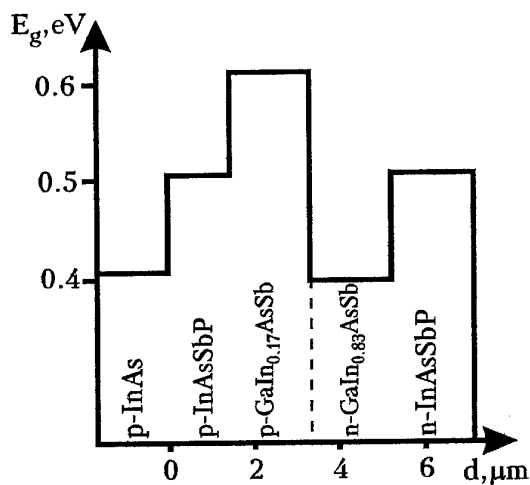


Figure 23 Novel tunneling-injection laser structure with type II broken-gap p-n GaInAsSb/InGaAsSb heterojunction in active region.

values of band-offsets in the conduction and valence bands ($\Delta E_C \sim 600$ meV, $\Delta E_V \sim 420$ meV). Mesa-stripe lasers had a stripe width $30 \mu\text{m}$ and cavity length $350 \mu\text{m}$. All kinds of these lasers were studied in pulse mode with pulse duration 100 ns and frequency 100 kHz in the temperature range 77 - 220 K. Temperature dependence of threshold current density, differential quantum efficiency and light polarization characteristics in spontaneous and coherent modes were also studied.

On type II GaInAsSb/InGaAsSb laser structure with broken-gap p-n junction in an active layer single mode coherent emission have been obtained at $\lambda = 3.18 \mu\text{m}$, and low

threshold current $J_{th} = 400 \text{ A/cm}^2$ was achieved, which was less by a factor five in comparison with preceding type II lasers based on p-p broken-gap heterojunction GaInAsSb/InAs, which was proposed and studied before.

Fig.24 represents threshold current temperature dependencies of two type II tunneling-injection laser structures with p-p or p-n broken-gap heterojunction in an active regions. In this novel laser structure a weaker temperature dependence of the threshold current density was observed up to 140 - 150 K, with high characteristic temperature $T_0 = 47$ K, as one can see in Fig.24 Maximum operation temperature 200 K in pulse mode was obtained in this novel laser design.

With temperature increase, threshold current density arises at $T \geq 150$ K (Fig.24). This fact can be due to contribution of CHHS Auger-recombination process, connected with spin-orbit splitting band, as well as intravalence band absorption. At higher temperature they can "kill" the lasing.

Light polarization was also measured in the p-n laser structure both in spontaneous and coherent emission mode. As it can be seen from Fig.25 TM-polarization prevails over TE-mode with current increasing. It confirms the optical tunneling origin of radiative recombination transitions on type II interface [35].

Let us discuss why a tunneling-injection laser with p-n junction in an active region can operate up to higher temperature than a laser based on p-p broken-gap heterojunction.

There are two main reasons of a weakening of threshold current dependence in the novel laser structure with p-n broken-gap heterojunction:

- radiative recombination in the p-p heterostructure under coherent generation condition takes place at the heterointerface. Due to non-threshold Auger-recombination process, minority carriers localize near the interface, and it leads to increasing of intravalence band absorption, which has a strong temperature dependence. It is one of the reasons of sharp threshold current dependence on temperature.
- the second negative factor which plays an important role in the p-p broken-gap structure is hole leakage current J_{thL} from wide-gap semiconductor through thin barrier at the interface. This current can dominate in total one, i.e. $J_L > J_R + J_A$.

In tunneling-injection laser based on type II broken-gap p-n heterojunction radiative recombination takes place in the interface on the side of n- narrow-gap semiconductor as it was shown by our electroluminescence studying at low temperatures. A temperature elevates holes concentration in n-type semiconductor increases essentially, as a result, radiative recombination rate R_{np} rises also. It is important to note that under coherent generation mode intraband absorption near the heterointerface becomes weaker due to less carrier concentration in comparison with one in n-semiconductor volume. At higher temperature ($T > 150K$) side by side with radiative recombination process at the interface Auger-recombination process in volume of InAs includes. It leads to more sharp temperature dependence of the threshold current in lasers with p-p junction in an active region than in devices with type II broken-gap p-n junctions.

In conclusion, we succeed in significant suppression of leakage current and prolongation of a weak temperature dependence of threshold current up to 150K

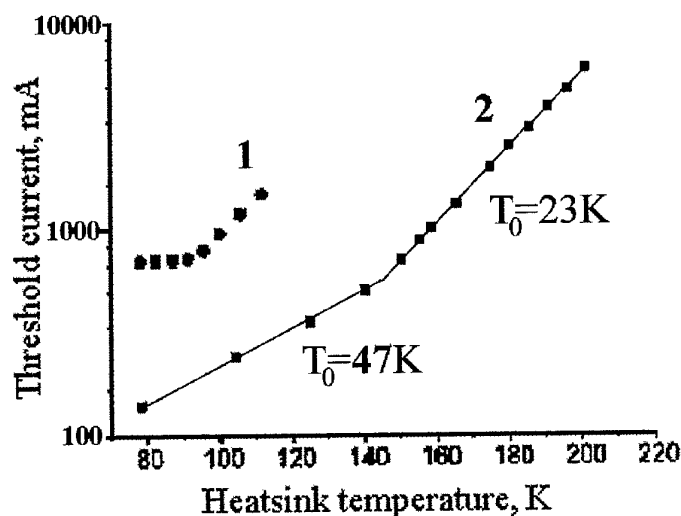


Figure 24 Temperature dependence of threshold current for novel tunneling-injection laser structure with type II broken-gap p-p and p-n GaInAsSb/InGaAsSb heterojunction in active regions.

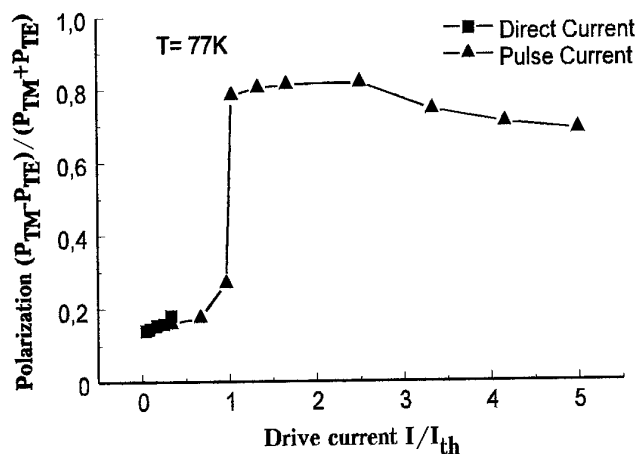


Figure 25 Light polarization of spontaneous and coherent emission from type II broken-gap p-n GaInAsSb/InGaAsSb heterolaser.

($T_0=47K$) due to using of type II p-n broken-gap heterojunction in active region of novel laser structure.

To improve laser performance and prolong the lasing up to room temperature the further optimization of laser structure is necessary. This process must include both fundamental physical mechanisms (such as suppression of Auger-recombination rate and intraband absorption) and modification of laser design, for example, with using novel non-injection quantum-well laser structures with asymmetric band offset confinement.

9.2 Spontaneous emission and superluminescence in AlGaAsSb/InAs/AlGaAsSb heterostructure.

Recently some investigators shown that using wide-gap confined layers with high Al content (up to 90%) led to essential improving of performance of infrared lasers [6,10]. But growing cladding layers AlGaAsSb with high Al content by LPE method on the narrow-gap semiconductors (InAsSb, InGaAsSb) represents not very simple task. In this work we succeeded in growing double heterostructure AlGaAsSb/InGaAsSb with high barrier heights.

Double heterostructure was grown on p-GaSb(100) substrate. As an active layer was chosen narrow-gap solid solution with high In content ($In_{0.90}Ga_{0.10}As_{0.89}Sb_{0.21}$ $E_g=326$ meV at 77 K) was chosen and $Al_{0.34}Ga_{0.66}As_{0.03}Sb_{0.97}$ cladding layers were grown. These wide-gap layers provide

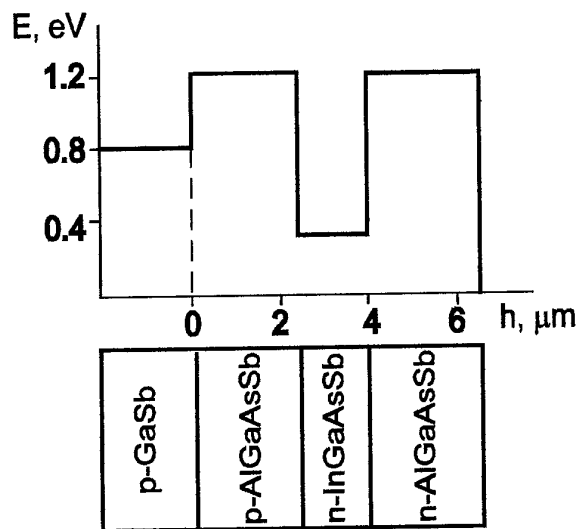


Figure 26 Schematic diagram of AlGaAsSb/InAs double heterostructure.

good electron confinement due to large band offset in the conduction band ($\Delta E_c \sim 1.0$ eV). It is important to note that this heterostructure was for the first time grown on the narrow-gap layer. Up to day growing narrow-gap solid solutions on the wide-gap ones is difficult due to bad matching of two materials with very different physical constants (e.g. thermal expansion coefficients). Growing temperature was 600°C . Narrow-gap InGaAsSb layers were grown on AlGaAs layers with lattice-mismatching less than 2.5×10^{-3} at $T=300$ K for compositions $0.01 < x < 0.1$, $y = x + 0.12$.

For wide-gap quaternary AlGaAsSb grown on GaSb substrate $\Delta a/a = (4-8) \times 10^{-4}$ were achieved. The thickness of the narrow-gap layer was $0.8-1.2 \mu\text{m}$, and of the wide-gap layers near $2.5 \mu\text{m}$. Carrier concentrations were $n, p \sim 5 \times 10^{16} \text{ cm}^{-3}$ in confined layers and $n \sim 1 \times 10^{17} \text{ cm}^{-3}$ for undoped active layer.

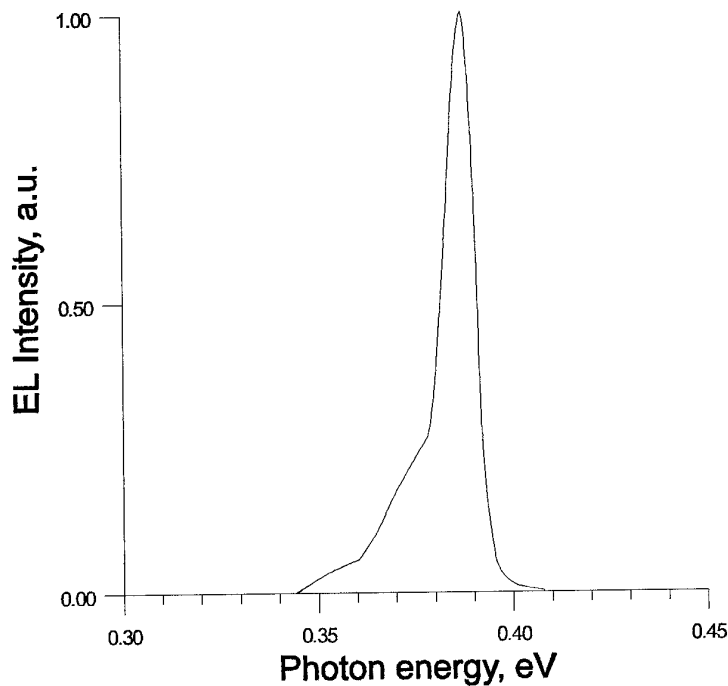


Figure 27 Emission of AlGaAsSb/InAs double heterostructure under superluminescence condition.

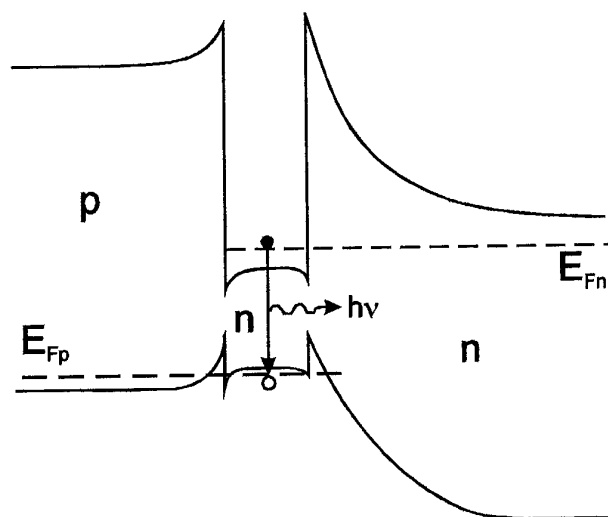


Figure 28 Energy band diagram of p-AlGaAsSb-n-InAs-n-AlGaAsSb heterostructure. Arrow shows a possible radiative recombination transition.

locked-in amplifier. To response registering LN₂ cooled InSb photoconductor was applied. Measurement were made in pulse mode with pulse duration 2.5 ms and reperion rate $f=10^5$ Hz.

Intensive spontaneous emission was found in the spectral range 3–4 μm (Fig.27), with the photon energy maximum $h\nu=387$ eV. Full width of half maximum FWHM was narrow, $\Delta h\nu=9-10$ meV. The spectrum of emission was asymmetric and has sharp shortwavelength edge. Intensity of the electroluminescence was comparable to one for conventional InAs/InAsP DH laser. Emission rises sharply at threshold voltage $V>\sim 0.8$ V.

It is interesting to notice that maximum photon energy 387 meV was higher than energy band gap of the narrow-gap active layer. ($E_g=326$ meV at $T=77$ K).

To explain obtained EL results let's consider energy band diagram of the heterostructure under study. As one can see from Fig.28, there is a high potential barrier for the electrons at the interface between the narrow-gap active layer and p-cladding layer, as well as at the n-N interface due to high band offset in conduction bands of AlGaAsSb and InGaAsSb. It increases a series resistance of the whole laser structure and turn on voltage. In this case depletion layer of space charge forms at the wide-gap semiconductor side and accumulation layer at the narrow-gap side. At the same time, large built-in potential confined holes in active layer of the double heterostructure.

So, quasi-Fermi levels for electrons and holes fall both in the conduction and valence bands of the narrow-gap layer. This energy band diagram can explain high

Fig.26 represents energy band of layer structure versus coordinate and sequence of layers. Mesa-stripe diode laser structures were made by standard photolithography method. Stripe width was 60–90 μm , cavity length $L=300-500$ μm . Ohmic contacts were fabricated from Au/Zn and Au/Te to the cap layer and substrate respectively by evaporation and then fusing in H₂ atmosphere.

Spontaneous emission was measured by using grating monochromator MDR-4 with

«blue» shift of the electroluminescence spectrum (up to 60 meV) in comparison with E_g value of narrow gap layer.

We can observe the superluminescence in AlGaAsSb/InGaAsSb DH. But we do not obtain lasing with further current increasing. We think that it connects with the insufficient optical confinement in this structure. Using additional confined layers GaSb or GaInAsSb allows us to improve the emission characteristics of this structure and to reach a lasing.

Comparative study of various types of InAs(Sb)/InAsSbP and GaInAsSb/InGaAsSbP laser heterostructures. Comparison with state-of-the-art mid-infrared lasers.

Comparative analysis of various types of lasers made in the frame of this Contract was performed. Some new approaches for laser design were proposed.

- i) Comparison of type I and type II conventional InAsSb/InAsSbP lasers shows that using type II heterostructure with high ratio of band offsets $\Delta E_v/\Delta E_c \sim 3$ leads to suppression of Auger-recombination in the region of high temperature ($T > 150$ K), and to decrease of the threshold current density and to increase of characteristic temperature T_0 in a factor of 1.5–2 ($T_0 = 40$ K) in comparison with type I InAs-based lasers ($T_0 = 23$ –30 K). Threshold current was decreased up to 12–14 mA at $T = 80$ K (in lasers with a stripe width 15 μm , cavity length 300 μm).
- ii) A new approach was developed for improving temperature performance of tunneling-injection lasers with the type II broken-gap heterojunction in an active layer. These lasers with p-p GaInAsSb/InAs heterojunction was proposed and realised in the frame of preceding EOARD Contract [32]. It operated in pulse mode at $\lambda = 3.2$ –3.4 μm up to $T = 77$ –125 K, threshold current value was $J_{th} = 2 \text{ kA/cm}^2$ at 77 K and characteristic temperature $T_0 = 60$ K was obtained in the range 77–110 K.

In the frame of this work we made advanced laser structure with improved temperature dependence of the threshold current. It was achieved due to using type II p-n broken-gap GaInAsSb/InGaAsSb heterojunction in an active layer. It allows to suppress hole leakage from the wide-gap quaternary layer and to raise operating temperature up to 200 K, with characteristic temperature $T_0 = 47$ K in the wider range 77–150 K. Threshold current density was decreased up to 200–400 A/cm^2 at $T = 80$ K.

- iii) Mid-ir lasers developed and studied in the frame of this Contract were grown by simple and cheap technological method of LPE and can be commercial available. They are up to standard with the best InAs(Sb)-based diode lasers made by MBE, MOCVD in the other scientific centres in the world (See for example [3-5]) as to their main performances (threshold current, operating temperature). Up to day quantum cascade lasers only can operate in pulse multi mode at room temperature. QCLs have high enough threshold current due to carrier heating problem [34]. But CW single mode operation of QCLs was obtained only up to 110 K ($\lambda=4.6 \mu\text{m}$). Total tuning range of 1.2 cm^{-1} was obtained only at 13 K. This laser can operate in pulse mode at 200 K.
- iv) As a great achievement one can consider fabrication a set of continuous wave high power single mode InAsSb/InAsSbP lasers for the spectral range $3.1\text{--}3.6 \mu\text{m}$ with good spectral and tuning performances (cw power up to 12 mW was achieved at 82 K, and tuning range up to 2 cm^{-1}) [21,22]. Such laser has a big field of application for gas monitoring pollutant, tunable laser diode spectroscopy, ecological monitoring. These lasers are unique for spectroscopic tasks in the mid-ir range and they are now out of competition.

Conclusion and outlook

In the frame of the Contract the following main results were reached:

1. Technology and new design of InAsSb(InAs)/InAsSbP laser heterostructures with separate electron and optical confinement and various band offsets $\Delta E_V/\Delta E_C$ ratio at the interface were developed. Improving temperature dependence of threshold current and increasing operation temperature was achieved for the first time in the lasers based on type II heterojunction with band offset $\Delta E_V/\Delta E_C \approx 3$. This experimental fact confirms theoretical prediction of Auger-recombination suppression in the type II heterojunction with high band offset ratio. The operation temperature 220 K and characteristic temperature $T_0=40K$ has achieved. The threshold current for InAsSb/InAsSbP laser was obtained as low as 12-14- mA at 77K (for stripe width 15 μm and cavity length 300 μm).
2. Continuous wave operation of InAsSb/InAsSbP laser structures were studied in details. Electrical properties, spectral and mode characteristics as well as long term stability were investigated.
CW high power, single mode InAsSb lasers with good performances operating up to 122K were developed. These devices are very promising for tunable diode laser spectroscopy and gas pollutant monitoring.
3. Theoretical analysis of non-radiative losses in longwavelength quantum well lasers was performed. It was established main factors limited high temperature performance of mid-ir lasers are leakage current, non-radiative Auger recombination losses, intravalence band absorption and effect of heating.
It was concluded that the suppression of Auger recombination and intravalence band absorption at the type II heterointerface is an important factor allowing to get a weaker temperature dependence of threshold current density in laser structure.
4. Electroluminescence of type II broken-gap p-n heterostructure GaInAsSb/InAs was studied under forward and reverse bias. Mechanism of negative differential resistance (NDR) and impact ionization at type II heterointerface was first proposed.
5. Advanced tunneling-injection laser based on type II broken-gap p-n GaInAsSb/InGaAsSb heterostructure was proposed and realized. Threshold

current about 200-400 A/cm² was obtained at 80K. Operation temperature near T=200K and characteristic temperature T₀=47 K were achieved.

6. AlGaAsSb/InAs double heterostructures were first grown lattice-matched to GaSb by LPE.

Spontaneous emission and superluminescence were studied. "Blue" shift of emission spectra was obtained due to strong electron confinement and Fermi-level lifting into conduction and valence bands of InAs active layer.

Some ways of further increasing the operating temperature of longwavelength lasers can be considered.

The first step is suppression of intravalence band absorption and non-radiative Auger-recombination losses in narrow-gap InAs-based semiconductor compound. It can be made by using GaSb-based solid solutions with a composition lying in the miscibility gap region (spinodal decomposition region) for an active layer. It allows to get longwavelength solid solutions with E_g out of resonance with spin-orbit splitting of the valence band. Another advantage of this method is the possibility for making quantum dots in an active layer and increase gain and quantum efficiency of longwavelength lasers. The second step consists of using the wide-gap emitter layers with small (~3-5kT) stepped variation of E_g versus coordinate in conduction and valence bands (stepped band offsets). It can lead to reducing carrier heating in active layer due to lowering barrier heights. Third, we have to overcome non-radiative recombination losses, intravalence band absorption in the active region and carrier heating. It may be done by a bandgap-engineering of some new laser designs.

The fourth way supposes the improving of hole confinement (electron confinement can be reached by high value of ΔE_c in type II heterojunctions). It can be reached, for example, by growing additional type II heterojunctions between active and cladding layers.

And at last, the majority of the mentioned above non-radiative losses can be overcome in a new designed non-injection quantum well laser with asymmetric band offset confinement. This construction combines some advantages of type I and type II intersubband lasers and will allow to reach larger gain (in 5-10 times) and weaker temperature dependence of the threshold current. Such laser structure can be grown from binary compound by MBE, MOCVD or mixed MBE—LPE technology.

References

1. HITRAN 92: L.S. Rothman, R.R. Gamache, R.H. Tipping, C.P. Rinsland, M.A.H. Smith, D. Chris Benner, V. Malathy Devi, J.-M. Flaud, C. Camy-Peyret, A. Perrin, A. Goldman, S.T. Massie, L.R. Brown, and R.A. Toth, "The HITRAN molecular database: editions of 1991 and 1992", *J. Quant. Spectrosc. Radiat. Transfer* 48, 469-507, 1992. L.R. Brown, R.H. Hunt, A.S. Pine, "Wavenumbers, Line Strengths, and Assignments in the Doppler-Limited Spectrum of Formaldehyde from 2700 to 3000 cm^{-1} ", *J. Molec. Spectrosc.* 75, 406-428, 1979
2. Schiff, G.I. Mackay and J. Bechara, "The Use of Tunable Diode Laser Absorption Spectroscopy for Atmospheric Measurements", in *Air Monitoring by Spectroscopic Techniques*, M.W. Sigrist, Editor, John Wiley & Sons, Inc., New York 1994.
3. D.H. Chow, R.H. Miles, T.G. Hasenberg, A.R. Kost, Y.H. Zhang, H.L. Dunlap, L. West. Mid-wave infrared diode lasers based on GaInAsSb/InAs and InAs/AlSb superlattices. *Appl. Phys. Lett.*, 67(25), 3700-3702 (1995).
4. A.A. Allerman, R.M. Biefeld, S.R. Kurtz. InAsSb-based mid-infrared lasers (3.8-3.9 μm) and light-emitting diodes with AlAsSb claddings and semimetal electron injection grown by metalorganic chemical vapor deposition. *Appl. Phys. Lett.*, 69(4), 465-467 (1996).
5. Menna, D.R. Capewell, R.U. Martinelli, P.K. York, R.E. Enstrom, "3.06 μm InGaAsSb/InPSb diode lasers grown by organometallic vapor-phase epitaxy", *Appl. Phys. Lett.* 59(17), 2127-2129, 1991.
6. K.D. Moiseev, M.P. Mikhailova, O.G. Ershov, Yu.P. Yakovlev Longwavelength laser ($\lambda=3.96 \mu\text{m}$) with isolated type II p-GaInAsSb/p-InAs single heterojunction in active region. *Techn. Phys. Lett.* 21 12 (1995).
7. J. Faist, F. Capasso, C. Sirtori, D.L. Sirco, A.L. Hutchinson, A.Y. Cho. Room-temperature mid-infrared quantum cascade lasers. *Electronics Lett.*, 32(6), 560-561 (1996).
8. J. Faist, F. Capasso, C. Sirtori, D.L. Sirco, A.L. Hutchinson, A.Y. Cho. "Continuous wave operation of a vertical transition quantum cascade laser above $T=80 \text{ K}$ ". *Appl. Phys. Lett.*, 67(22), 3057-3059 (1995).
9. Lee G.W., Turner J.R., Ochoa A., Sanchez "High-efficiency, high-temperature mid-infrared ($\lambda=4 \mu\text{m}$) InAsSb/GaSb lasers", *Electron. Lett.* 23, 1944-1945, 1994.

10. Eglash, H.K. Choi, "InAsSb/AlAsSb double heterostructure diode lasers emitting at 4 μm ", Appl. Phys. Lett. 64(7), 833-835, 1994.
11. H.K. Choi, G.W. Turner, H.Q. Lee. InAsSb/InAlAs strained quantum-well lasers emitting at 4.5 μm . Appl. Phys. Lett., 66(26), 3543-3545 (1995).
12. H.K. Choi, G.W. Turner, M.J. Manfra, M.K. Connors. 175 K continuous wave operation of InAsSb/InAlAsSb quantum-well diode lasers emitting at 3.5 μm . Appl. Phys. Lett., 68(21), 2936-2938 (1996).
13. Z. Feit, M. McDonald, R.J. Woods, V. Archambault, P. Mak. Low threshold PbEuSeTe/PbTe separate confinement buried heterostructure diode lasers. Appl. Phys. Lett., 68(6), 738-740 (1996).
14. Z. Feit, D. Kostyk, R.J. Woods, P. Mak. Molecular beam epitaxy grown PbEuSeTe buried heterostructure lasers with continuous wave operation at 195 K. Appl. Phys. Lett., 57(15), 2891-2893 (1990).
15. Xu, A. Lambrecht, M. Tacke, "Lead chalcogenide implanted diode lasers in CW operation above 77 K", Electron. Lett. 30(7), 571-573, 1994.
16. R.Q. Yang and S.S. Pei. Novel type II quantum cascade lasers. J. Appl. Phys., 79(11), 8197-8203 (1996).
17. Baranov, A.N. Imenkov, V.V. Sherstnev, Y.P. Yakovlev, "2.7-3.9 μm InAsSb(P)/InAsSbP low threshold diode lasers", Appl. Phys. Lett., 64(19), 2480-2481, 1994.
18. Popov, V. Sherstnev, Y. Yakovlev, R. Mücke, P. Werle, "High power InAsSb/InAsSbP double heterostructure laser for continuous wave operation at 3.6 μm ", Appl. Phys. Lett. 68(20), 2790-2792, 1996.
19. Choi, G.W. Turner, M.J. Manfra, "High-power (>200 mW/facet) at 3.4 μm from InAsSb/InAlAsSb strained quantum well diode lasers", Electron. Lett. 32(14), p.1296-1297, 1996.
20. A. Popov, V. Sherstnev, Y. Yakovlev, R. Mücke, B. Sheumann, P. Werle, "InAssb/InAsSbP double heterostructure laser emitting at 3.4 μm ", Infrared Physics and Technology, A52(8), 863-870, 1996.
21. A. Popov, V. Sherstnev, Y. Yakovlev, R. Mücke, P. Werle, "Single-frequency InAssb/InAsSbP double heterostructure laser emitting at 3.4 μm ", Spectrochimica Acta A52(8), 863-870, 1996.
22. A. Popov, V. Sherstnev, Y. Yakovlev, R. Mücke, P. Werle, "Tuning and spectral performance of mid-infrared InAsSb lasers", Proc. SPIE 2834, pp.46-56, 1996.
23. Mani, A. Joulie, "Some characteristics of 3.2 μm injection lasers based on InAsSb/InAsSbP system", Proc. SPIE 1362, pp.38-48, 1990.
24. G.G. Zegrya, A.D. Andreev, Mechanism of suppression of Auger recombination in type II heterostructures. Appl. Phys. Lett. 67, 2681 (1995).

25. G.G.Zegrya in book: Antimonide-related strained layer heterostructures, Ed. By M.O.Manasreh, Gordon and Breach, Neward, 1997 (in print).
26. M.Aydaraliev, G.G.Zegrya, N.V.Zotova, S.A.Karandashov, B.A.Matveev, N.M.Stus', G.N.Talalakin, " The nature of temperature dependence of threshold current density of long-wave lasers based on InAsSbP/InAs and InAsSbP/InAsSb DH", Semiconductors, 26(2), pp.246-256, 1992.
27. N.M.Kolchanova, A.A.Popov, A.B.Bogoslovskaya, G.A.Sukach, Nonequilibrium heating in GaInAsSb heterostructures, Tech. Phys. Lett. **19** 690 (1993).
28. V.L.Gelmont and Z.N.Sokolova, Auger recombination in n-type direct-gap semiconductors, Sov. Phys. Semicond., 16 1067 (1982).
29. J.Faist, F.Capasso, C.Sirtori, D.Sivco, A.L.Hutchinson, S.-N.G.Chu, A.Y.Cho Continuous wave operation of quantum cascade lasers based on vertical transitions at $\lambda=4.6 \mu\text{m}$.
30. M.P.Mikhailova, K.D.Moiseev, I.N.Timchenko, O.G.Ershov, G.G.Zegrya, Yu.P.Yakovlev Observation of electroluminescence of confined carriers at the type II broken-gap p-GaInAsSb/p-InAs single heterojunction. Semiconductors, (1995).
31. K.D.Moiseev, M.P.Mikhailova, O.G.Ershov, Yu.P.Yakovlev Tunnel-injection laser based on a single p-GaInAsSb/p-InAs type II broken-gap heterojunction. Semiconductors, **30**, 3, p.223-225 (1996).
32. Final report on EOARD Contract F6 170894 C0011, Ioffe Institute, St.Petersburg.
33. M.P.Mikhailova, K.D.Moiseev, O.G.Ershov, G.G.Zegrya, Yu.P.Yakovlev Tunneling-injection laser based on type II broken-gap p-GaInAsSb/p-InAs heterojunction. Proceed. Of ISDRS-95, Charlottesville, VA, December 1995, p.421-424..
34. V.Gorfinkel, S.Luryi Temperature dependence of the characteristics of quantum cascade lasers. Appl. Phys. Lett. (1995).
35. N.S.Averkiev, A.N.Baranov, A.N.Imenkov, A.A.Rogachev, Yu.P.Yakovlev Sov.Tech.Phys.Lett. **13** 332 (1987).

Papers published in the frame of this Contract

- 1*. T.N.Danilova, A.P.Danilova, O.G.Ershov, A.N.Imenkov, N.M.Kolchanova, M.V.Stepanov, V.V.Sherstnev, Yu.P.Yakovlev "Diode lasers with separate electrical and optical confinement based on InAsSb and radiating in range 3-4 μm "-Semiconductors v.31, 1997 (in print).
- 2*. Yu.P.Yakovlev, T.N.Danilova, A.N.Imenkov, M.P.Mikhailova, K.D.Moiseev, O.G.Ershov, V.V.Sherstnev, G.G.Zegrya "Suppression of Auger recombination in the diode lasers based on type II InAsSb/InAsSbP and InAs/GaInAsSb heterostructures" - SPIE vol3001 In plane Semiconductor Lasers from Ultraviolet to Mid-Infrared. (in print). Photonic West-97. Optoelectronics'97.
- 3*. K.D.Moiseev, M.P.Mikhailova, O.V.Andreychuk, B.E.Samorukov, Yu.P.Yakovlev "Superluminescence in GaAlAsSb/InAs double heterostructure" - Techn.Phys.Lett., v.23, (in print) 1997.
- 4*. V.A.Solov'ev, M.P.Mikhailova, M.V.Stepanov, V.V.Sherstnev, Yu.P.Yakovlev "New possibility of scanning electron microscopy for studying InAsSb/InAsSbP lasers"- Techn.Phys.Lett., (in print) 1997.
- 5*. K.D.Moiseev, M.P.Mikhailova, O.G.Ershov, Yu.P.Yakovlev "Infrared laser ($\lambda=3.2 \mu\text{m}$) based on type II broken-gap heterojunction with improved temperature performance"- Techn.Phys.Lett., v.23, N5, 1997.
- 6*. Yu.P.Yakovlev, T.N.Danilova, A.N.Imenkov, O.G.Ershov, K.D.Moiseev, M.P.Mikhailova, V.V.Sherstnev "Mid infrared diode lasers based on III-V compounds for the spectral range 3-4 μm (invited paper) Proceed. 23 Intern. Symp.Comp.Semicond.St.-Petersburg, Russia, 22-27 Sept 1996, IOPP publ. in print
- 7*. Yu.P.Yakovlev, K.D.Moiseev, M.P.Mikhailova, O.G.Ershov, G.G.Zegrya "Advanced tunnel-injection laser based on the type II broken-gap p-n GaInAsSb/ InAs heterojunction for the spectral range 3-3.5 μm " -Technical Digest CLEO-96, Anaheim, Calif., June 2-7, 1996, p.170-171.
- 8*. T.N.Danilova, A.N.Imenkov, O.G.Ershov, M.V.Stepanov, V.V.Sherstnev, Yu.P.Yakovlev "Maximum operating temperature of InAsSb/InAsSbP diode lasers" Semiconductors, v.30(7), p.667-670 (1996).
- 9*. T.N.Danilova, A.P. Danilova, O.G.Ershov, A.N.Imenkov, M.V.Stepanov, V.V.Sherstnev, Yu.P.Yakovlev "Current tuning of low-threshold mesa-stripe InAsSb/InAsSbP double heterostructure lasers in the spectral region near 3.3 μm "- Semiconductors, v.31(6), (1997), in print.

- 10*. A.V.Gorbatyuk, G.G.Zegrya, K.D.Moiseev, M.P.Mikhailova, O.V.Andreychuk, N.D.Stoyanov, Yu.P.Yakovlev "Negative Differential resistance and radiative recombination in type II broken-gap p-GaInAsSb/p-InAs single heterojunctions"- Abstract of Invited Lectures and Contributed Papers of Int.Symp. "Nanostructures: Physics and Technology", St.Petersburg, Russia, 24-28 June, 1996, p.62.
- 11*. G.G.Zegrya, N.V.Zotova, Z.N.Sokolova, N.M.Stus', V.B.Khalfin, Yu.P.Yakovlev "A study of of intravalence band absorption in the valence band of III-V narrow-gap semiconductors and its influence on longwavelength lasers performance"- Semiconductors, v.31(6), (1997), in print.

For remarks
